

Superstring Z' boson in e^-e^+ annihilation

S. K. Abdullaev and A. I. Mukhtarov
Baku State University, Baku, Azerbaidzhan

Fiz. Élem. Chastits At. Yadra **26**, 1264–1321 (September–October 1995)

In the framework of the $SU(2) \times U(1)$ and $SU(2) \times U(1) \times U'(1)$ gauge models, the processes $e^-e^+ \rightarrow ff$, $e^-e^+ \rightarrow \tilde{f}\tilde{f}$, $e^-e^+ \rightarrow q\bar{q}g$, $e^-e^+ \rightarrow \tilde{q}\tilde{q}g$, $e^-e^+ \rightarrow e^-e^+$, $e^-e^- \rightarrow e^-e^-$, $e^-e^+ \rightarrow BX$ are studied. Expressions are obtained for the helicity amplitudes and the effective cross sections. The following characteristics are considered: the right–left asymmetry A_{RL} , the forward–backward asymmetry A_{FB} , the forward and backward polarization asymmetries $A_F(\lambda_2)$ and $A_B(\lambda_2)$, the forward–backward polarization asymmetry $\tilde{A}_{FB}(\lambda_2)$, the degree of fermion longitudinal polarization P , the transverse spin asymmetry $A_\phi^{(1)}$, etc. Expressions are obtained for these characteristics, and quantitative estimates are obtained for them in the framework of the standard model and the E_6 superstring model. The zeros of the helicity amplitudes and of the electroweak asymmetries are discussed. © 1995 American Institute of Physics.

INTRODUCTION

In the development of modern elementary-particle physics, study of inelastic lepton–nucleon scattering and the annihilation of colliding electron–positron beams has played an important role. Indeed, these experiments, made at ever increasing energies, led to the discovery of most of the effects that have played an important role in our understanding of the nature of fundamental interactions and the structure of elementary particles. For example, the scaling discovered in deep inelastic lepton–nucleon scattering and the jet picture of inclusive hadron production in electron–positron annihilation led to the creation of the quark–parton model of the hadrons and then to the quantum-chromodynamical theory of the strong interaction.

The experimental investigation of electron–positron annihilation into hadrons proved to be remarkably fruitful for elementary-particle physics. In a brief period, these experiments led to the discovery of whole families of hadronic resonances ψ and Y , for the description of which it was necessary to introduce the heavy c and b quarks with the new quantum numbers charm and beauty. Study of the levels of “charmonium” and “beautonium,” and also their decays made it possible to test several predictions of quantum chromodynamics (QCD), to estimate the value of an important parameter such as the strong coupling constant α_s , and to establish convincing evidence for the existence of the vector gluon.

One of the most important discoveries in the field of the weak interactions was that of the weak neutral currents, which was made in 1973 at CERN in the bubble chamber Gargamelle. Even before this experiment, Glashow, Weinberg, and Salam (GWS)¹ had constructed a model of a unified theory of the weak and electromagnetic interactions that predicted the existence of the weak neutral currents. After their experimental discovery, study of the structure of these currents occupied a central position in experimental and theoretical studies.^{2–7} Investigation of the effects of the weak neutral currents in different laboratories in the world convincingly confirmed the correctness of the standard model,

but, nevertheless, comprehensive testing of it continues.⁸

Despite the successes of the GWS theory, there are reasons for being unsatisfied with the standard model. For example, the reasons for the repetition of the generations of leptons and quarks are unclear, there is no explanation of their number, the mechanism of generation of the particle masses is unknown, and there is no theoretical derivation of their spectrum. The existence of the scalar Higgs boson has not yet been proved, and the t quark has not been discovered. The space–time structure of the weak interactions does not follow from any internal requirements of the theory but is introduced phenomenologically in accordance with experimental facts. Several parameters of the standard model are known with insufficient accuracy.

All these circumstances indicate the need for deeper testing of the standard model and also for a more general theory capable of eliminating the phenomenological features of the existing model.

A great achievement of recent years in the development of high-energy physics is the development of superstring theory.⁹ The superstring model of elementary particles based on the $E_8 \times E'_8$ gauge symmetry is regarded as a real candidate for a consistent unified theory of all the fundamental interactions, including gravity.¹⁰ After compactification, the 10-dimensional $E_8 \times E'_8$ superstring group leads to the 4-dimensional $N=1$ supersymmetric theory with gauge group E_6 . The observed matter fields are then grouped in E_6 27-plets. An interesting consequence of this model is that it predicts the existence of new exotic fermions and at least one additional vector boson Z' with a mass below 1 TeV (Ref. 11). The existence of the additional Z' boson must lead to a characteristic deviation of experimental results from the standard model in all processes due to weak neutral currents.

Therefore, going over to higher energies and larger momentum transfers, we hope to discover signals of a “new physics.” It is this circumstance that is stimulating the high-precision measurements of the parameters of the standard model.⁸ The possibility of interpreting deviations from the standard model as indications of a superstring Z' boson re-

TABLE I. Quantum numbers of the fields of the E_6 27-plet [$Q_i(\psi_R) = -Q_i(\psi_L)$].

$SO(10)$	$SU(5)$	$SU_c(3)$	Left field	I_{3L}	Q_f	$2\sqrt{15}Q_\eta$	$2\sqrt{10}Q_\chi$	$\sqrt{24}Q_\psi$
16	$\bar{5}$	$\bar{3}$	d^c	0	1/3	1	3	1
		1	e^-	-1/2	-1	1	3	1
		1	ν_e	1/2	0	1	3	1
		1	e^{-c}	0	1	-2	-1	1
		3	d	-1/2	-1/3	-2	-1	1
	10	$\bar{3}$	u	1/2	2/3	-2	-1	1
		3	u^c	0	-2/3	-2	-1	1
		1	ν^c	0	0	-5	-5	1
		$\bar{5}$	h^c	0	1/3	1	-2	-2
		1	E^-	-1/2	-1	1	-2	-2
10	$\bar{5}$	1	ν_E	1/2	0	1	-2	-2
		3	h	0	-1/3	4	2	-2
		1	E^{-c}	1/2	1	4	2	-2
	5	1	N_E^c	-1/2	0	4	2	-2
		1	n	0	0	-5	0	4
		1						
1	1	1						

quires study of a large class of processes in which the Z' boson participates.

Currently, much attention is being devoted to searches for manifestations of an additional vector boson.¹²⁻¹⁹ One of the effective methods is to study electroweak asymmetries in electron-positron annihilation at energies $\sqrt{s} \geq 100$ GeV. In Refs. 20-29, we obtained general expressions for the various integrated characteristics of the reactions $e^-e^+ \rightarrow f\bar{f}$, $e^-e^+ \rightarrow f\bar{f}$, $e^-e^+ \rightarrow q\bar{q}g$, $e^-e^+ \rightarrow \bar{q}qg$, $e^-e^+ \rightarrow e^-e^+$, $e^-e^+ \rightarrow e^-e^+$, $e^-e^+ \rightarrow BX$, $e^-e^+ \rightarrow \gamma X$ and made a detailed analysis of these characteristics in the framework of the standard model and the E_6 superstring model.

In this paper, we give a brief review of the results of the investigation of the effects of the superstring Z' boson in the production of particles in electron-positron annihilation.

1. NEUTRAL CURRENTS IN THE E_6 SUPERSTRING MODEL

In the low-energy superstring limit, the symmetry of the E_6 group can be broken in accordance with the scheme

$$E_6 \rightarrow SO(10) \times U_\psi(1).$$

The group $SO(10)$ contains $SU(5)$ as a subgroup. The breaking of $SO(10)$ takes the form

$$SO(10) \rightarrow SU(5) \times U_\chi(1),$$

with

$$SU(5) \rightarrow SU_c(3) \times SU_L(2) \times U_Y(1).$$

Therefore, the group E_6 can be broken down to subgroups of fifth or sixth rank:

$$G_5 = SU_c(3) \times SU_L(2) \times U_Y(1) \times U_\eta(1) \quad (1.1)$$

$$G_6 = SU_c(3) \times SU_L(2) \times U_Y(1) \times U_\psi(1) \times U_\chi(1). \quad (1.2)$$

In G_5 , there necessarily arises one additional (compared with the standard model) neutral bosonic field Z_η corresponding to the $U_\eta(1)$ symmetry. In the group G_6 we have two additional neutral bosons Z_ψ and Z_χ corresponding to the

subgroups $U_\psi(1)$ and $U_\chi(1)$, respectively. However, it is assumed that there exists an intermediate scale $M_I \approx 10^{10-11}$ GeV at which one of these fields acquires a mass $M \approx M_I$ by spontaneous symmetry breaking. Such breaking may be induced by nonvanishing vacuum expectation values of scalar superpartners ν^c and n in the E_6 27-plet. As a result, in this case too, there remains only one light ($M < 1$ TeV) Z' boson.¹¹

The model with gauge group $SU_L(2) \times U_Y(1) \times U'(1)$ is currently assumed to be the most probable low-energy limit of superstring theory. In this model, there arises an additional Z' boson, which is regarded as a linear combination of Z_ψ and Z_χ :

$$Z' = Z_\psi \cos \theta_E + Z_\chi \sin \theta_E. \quad (1.3)$$

Here θ_E is the mixing angle, which is determined by the scheme of the symmetry breaking at the intermediate scale. In the case of a group of rank 6, the angle θ_E is arbitrary, but for the group G_5 it is $\theta_E = 142.24^\circ$. The values of the angle $\theta_E = 0^\circ$ and 90° correspond to the pure states Z_ψ and Z_χ . The angles $\theta_E = -\tan^{-1}(3/5)^{1/2}$ and $\theta_E = -\tan^{-1}(5/3)^{1/2}$ describe the Z_η and Z_I bosons.¹³

The eigenvalues of the generators of the groups $U_\eta(1)$, $U_\chi(1)$, and $U_\psi(1)$ for the fields in the E_6 27-plet are given in Table I.

To the additional Z' boson (3) there corresponds the generator

$$Q_{Z'} = Q_\psi \cos \theta_E + Q_\chi \sin \theta_E, \quad (1.4)$$

where Q_ψ and Q_χ are the generators of $U_\psi(1)$ and $U_\chi(1)$.

The Lagrangian of the interaction of the fundamental fermions with the gauge bosons has the form

$$\mathcal{L} = \frac{e}{2} [J_\mu^\gamma A_\mu + J_\mu^Z Z_\mu + J_\mu^{Z'} Z'_\mu], \quad (1.5)$$

where

$$J_\mu^i = \bar{\psi}_f \gamma_\mu [g_{L_f}^i (1 + \gamma_5) + g_{R_f}^i (1 - \gamma_5)] \psi_f \quad (1.6)$$

in which g_{Lf}^i and g_{Rf}^i are the chiral coupling constants of the fermion f with the gauge bosons i ($i = \gamma, Z, Z'$), the values of which are

$$\begin{aligned} g_{Lf}^\gamma &= g_{Rf}^\gamma = Q_f, & g_{Lf}^Z &= \frac{2}{\sin 2\theta_w} (I_3^f - Q_f x_w), \\ g_{Rf}^Z &= \frac{2}{\sin 2\theta_w} (-Q_f x_w), \\ g_{Lf}^{Z'} &= \sqrt{\frac{5}{3}} \cdot \frac{1}{\cos \theta_w} [Q_\psi(f_L) \cos \theta_E + Q_x(f_L) \sin \theta_E], \\ g_{Rf}^{Z'} &= \sqrt{\frac{5}{3}} \cdot \frac{1}{\cos \theta_w} [-Q_\psi(f_L^c) \cos \theta_E - Q_x(f_L^c) \sin \theta_E]. \end{aligned} \quad (1.7)$$

Here $x_w = \sin^2 \theta_w$ is the Weinberg angle, and Q_f and I_3^f are the electric charge and the third projection of the weak isospin of the fermion f .

In the general case, the mass matrix of the fields Z and Z' is nondiagonal:

$$M^2 = \begin{pmatrix} M_Z^2 & \delta M^2 \\ \delta M^2 & M_{Z'}^2 \end{pmatrix}. \quad (1.8)$$

This leads to Z - Z' mixing. As a result of the diagonalization of the matrix (1.8), we find the fields Z_1 and Z_2 :

$$\begin{pmatrix} Z_1 \\ Z_2 \end{pmatrix} = \begin{pmatrix} \cos \Phi & \sin \Phi \\ -\sin \Phi & \cos \Phi \end{pmatrix} \begin{pmatrix} Z \\ Z' \end{pmatrix} \quad (1.9)$$

with definite masses M_{Z_1} and M_{Z_2} , which, like the mixing angle Φ , can be expressed in terms of the original parameters:

$$\begin{aligned} M_{Z_1}^2 &\approx M_Z^2 - \frac{(\delta M^2)^2}{M_{Z'}^2 - M_Z^2}, \\ M_{Z_2}^2 &= M_{Z'}^2 + \frac{(\delta M^2)^2}{M_{Z'}^2 + M_Z^2} \tan^2 \Phi = (M_Z^2 - M_{Z_1}^2) / (M_{Z_2}^2 - M_Z^2). \end{aligned} \quad (1.10)$$

In the E_6 superstring model with intermediate group G_5 , there are two $SU_L(2)$ doublets (H, \bar{H}) and one singlet N of Higgs fields. In this case,

$$\delta M^2 = M_Z^2 x_w \frac{4v^2 - \bar{v}^2}{3(v^2 + \bar{v}^2)}, \quad M_{Z'}^2 = M_Z^2 \frac{16v^2 + \bar{v}^2 + 25x^2}{9(v^2 + \bar{v}^2)}, \quad (1.11)$$

where $v = \langle H^0 \rangle \equiv \langle \tilde{N}_E^c \rangle$, $\bar{v} = \langle \bar{H}^0 \rangle \equiv \langle \tilde{\nu}_E \rangle$, $x = \langle N \rangle \equiv \langle \tilde{n} \rangle$; \tilde{N}_E , $\tilde{\nu}_E$, and \tilde{n} are the scalar superpartners of the corresponding fermions in the 27-plet. Such a structure of the Higgs fields leads to the following restriction on the mixing angle Φ (Ref. 30):

$$-\frac{8}{3} \frac{x_w}{M_{Z_2}^2 / M_Z^2 - 1} < \tan 2\Phi < \frac{2}{3} \frac{x_w}{M_{Z_2}^2 / M_Z^2 - 1}. \quad (1.12)$$

The expression for the Lagrangian of the interaction of the fermions with the gauge bosons Z_1 and Z_2 follows from (1.5):

$$\mathcal{L} = \frac{e}{2} (J_\mu^{Z_1} Z_{1\mu} + J_\mu^{Z_2} Z_{2\mu}), \quad (1.13)$$

where the currents $J_\mu^{Z_1}$ and $J_\mu^{Z_2}$ have the general form (6), but at the same time

$$\begin{aligned} g_{L(R)f}^{Z_1} &= \cos \Phi \cdot g_{L(R)f}^Z + \sin \Phi \cdot g_{L(R)f}^{Z'}, \\ g_{L(R)f}^{Z_2} &= -\sin \Phi \cdot g_{L(R)f}^Z + \cos \Phi \cdot g_{L(R)f}^{Z'}. \end{aligned} \quad (1.14)$$

The weak neutral current of the fermion f can also be represented in the form

$$J_\mu^i = \bar{\psi}_f \gamma_\mu (g_{Vf}^i + \gamma_5 g_{Af}^i) \psi_f, \quad (1.15)$$

where

$$g_{Vf}^i = g_{Lf}^i + g_{Rf}^i, \quad g_{Af}^i = g_{Lf}^i - g_{Rf}^i \quad (1.16)$$

are the vector and axial constants of the weak neutral current of the fermion.

2. HELICITY AMPLITUDES AND ELECTROWEAK ASYMMETRIES OF THE PROCESSES $e^-e^+ \rightarrow f\bar{f}$ AND $e^-e^+ \rightarrow f\bar{f}$

The annihilation of an electron-positron pair into various particles can proceed not only by means of a photon γ and a Z^0 boson but also by means of the additional Z' boson. The presence in the intermediate states of massive particles leads to a change of the energy dependence of the cross section and to the appearance of some specific P -odd asymmetries associated with the existence of an axial component of the weak neutral currents. Investigation of these effects in colliding e^-e^+ beams can help in the study of the properties of the weak neutral currents of both the initial and the final particles.

At the present time, experiments performed with the PEP, PETRA, and TRISTAN e^-e^+ beams have made it possible to study the effects of the neutral currents in $e^-e^+ \rightarrow \mu^-\mu^+$, $e^-e^+ \rightarrow \tau^-\tau^+$, $e^-e^+ \rightarrow e^-e^+$, and $e^-e^+ \rightarrow q\bar{q}$ annihilation processes at energies $\sqrt{s} \sim 30$ –60 GeV (Refs. 31–35). The SLC and LEP facilities with colliding e^-e^+ beams have recently been commissioned and have provided some data in measurements of the parameters of the standard boson in the region of the Z resonance ($\sqrt{s} \sim 90$ GeV).^{36–44} Measurements have been made of the mass and of the total and partial decay widths of the Z boson, and the coupling constants of the weak neutral currents of the leptons and quarks with the Z boson have been extracted. The results of these experiments are in satisfactory agreement with the predictions of the standard model.

From the point of view of obtaining information about the properties of the superstring Z' boson, huge interest attaches to study of the polarization characteristics of the particles (leptons, baryons, vector mesons) produced in electron-positron annihilation. Programs for new high-precision experiments to test the standard model using polarized e^-e^+ beams have recently been prepared in joint studies in American and European accelerator centers.⁴⁵ These programs will make it possible to study in detail various polarization characteristics in particle production in e^-e^+

annihilation, and this will make it possible to solve many important problems in the physics of the electroweak interactions at high energies.

We discuss here some qualitative properties of the helicity amplitudes and electroweak asymmetries of processes of annihilation of an e^-e^+ pair into a pair of fundamental fermions (leptons, quarks) and scalar fermions:

$$e^- + e^+ \rightarrow (\gamma, Z_1^0, Z_2^0, \dots) \rightarrow f + \bar{f}, \quad (2.1)$$

$$e^- + e^+ \rightarrow (\gamma, Z_1^0, Z_2^0, \dots) \rightarrow \tilde{f} + \bar{\tilde{f}}. \quad (2.2)$$

In the lowest order of perturbation theory, the process (2.1) is described by the matrix element

$$M = e^2 \sum_i D_i(s) \bar{v} \gamma_\mu [g_{Le}^i (1 + \gamma_5) + g_{Re}^i (1 - \gamma_5)] u \bar{u}_f \gamma_\mu [g_{Lf}^i (1 + \gamma_5) + g_{Rf}^i (1 - \gamma_5)] v_f, \quad (2.3)$$

where the summation is over all the gauge bosons ($i = \gamma, Z_1, Z_2, \dots$); $D_i(s) = (M_i^2 - s - iM_i\Gamma_i)^{-1}$ is the propagator of the vector boson i ; M_i and Γ_i are the mass and total width of the boson i ; s is the square of the total energy of the e^-e^+ pair in the center-of-mass system; and g_{Le}^i (g_{Lf}^i) and g_{Re}^i (g_{Rf}^i) are the left and right coupling constants of the electron (respectively, fermion) with the gauge boson i (they are given in Sec. 1).

We first discuss some qualitative properties of the processes (2.1) in the collision of longitudinally polarized electrons and positrons. The interaction of the fundamental fermions with the gauge bosons has vector and axial-vector components. This circumstance leads to conservation of the helicity of the fermions at high energies. The conservation of the helicity requires that the colliding electron and positron have opposite helicities ($e_L^-e_R^+$ or $e_R^-e_L^+$, where e_L^- is an electron with helicity -1 , e_R^+ is a positron with helicity $+1$, etc.). The same is true for the fermions in the final state. Therefore, for the reactions (2.1) there can arise only four independent helicity amplitudes F_{LL} , F_{LR} , F_{RL} , and F_{RR} (the first and second subscripts correspond to the helicities of the electron and the fermion f), which describe the following processes:

$$e_L^- + e_R^+ \rightarrow f_L + \bar{f}_R, \quad e_L^- + e_R^+ \rightarrow f_R + \bar{f}_L,$$

$$e_R^- + e_L^+ \rightarrow f_L + \bar{f}_R, \quad e_R^- + e_L^+ \rightarrow f_R + \bar{f}_L.$$

The differential cross sections corresponding to these four processes are²³

$$\frac{d\sigma}{d\Omega} (e_L^- e_R^+ \rightarrow f_L \bar{f}_R) = \frac{\alpha^2}{4} N_c s |F_{LL}|^2 (1 + \cos \theta)^2,$$

$$\frac{d\sigma}{d\Omega} (e_L^- e_R^+ \rightarrow f_R \bar{f}_L) = \frac{\alpha^2}{4} N_c s |F_{LR}|^2 (1 - \cos \theta)^2,$$

$$\frac{d\sigma}{d\Omega} (e_R^- e_L^+ \rightarrow f_L \bar{f}_R) = \frac{\alpha^2}{4} N_c s |F_{RL}|^2 (1 - \cos \theta)^2,$$

$$\frac{d\sigma}{d\Omega} (e_R^- e_L^+ \rightarrow f_R \bar{f}_L) = \frac{\alpha^2}{4} N_c s |F_{RR}|^2 (1 + \cos \theta)^2.$$

Here

$$F_{AB} = \sum_i D_i(s) g_{Ae}^i g_{Bf}^i \quad (A, B = L, R) \quad (2.4)$$

are the helicity amplitudes, N_c is the color factor ($N_c = 3$ for quarks and $N_c = 1$ for leptons), and θ is the angle between the momenta of the fermion and the electron.

The helicity amplitudes of the processes (2.1) in the standard model are determined by the expressions

$$F_{AB}^{(SM)} = \frac{Q_f}{s} + D_Z(s) g_{Ae}^Z g_{Bf}^Z \quad (A, B = L, R). \quad (2.5)$$

It is easy to show that in the limit of zero width of the Z boson the helicity amplitudes (2.5) have zeros at certain energies of the colliding e^-e^+ beams.^{23,27} The amplitudes $F_{LR}^{(SM)}$ and $F_{RR}^{(SM)}$ vanish at the energies $\sqrt{s} = \sqrt{2} M_Z \cos \theta_w$ and $\sqrt{s} = M_Z \cos \theta_w$, irrespective of the nature of the produced $f\bar{f}$ pair.

The helicity amplitudes $F_{RL}^{(SM)}$ and $F_{LL}^{(SM)}$ have zeros when the e^-e^+ beams have energies

$$\sqrt{s} = M_Z \cos \theta_w [Q_f / (Q_f - I_3^f)]^{1/2}$$

and

$$\sqrt{s} = \frac{1}{2} M_Z \sin 2\theta_w \left[Q_f / \left(x_w \left(\frac{1}{2} Q_f - I_3^f \right) + \frac{1}{2} I_3^f \right) \right]^{1/2},$$

respectively. In particular, for the production of a lepton pair $\mu^- \mu^+$ ($\tau^- \tau^+$)

$$F_{RL}^{(SM)} = 0 \quad \text{for} \quad \sqrt{s} = \sqrt{2} M_Z \cos \theta_w,$$

$$F_{LL}^{(SM)} = 0 \quad \text{for} \quad \sqrt{s} = M_Z \sin 2\theta_w.$$

We denote by λ_1 (η_1) and λ_2 (η_2) the values of the longitudinal (respectively, transverse) polarizations of the electron and the positron, and by h_1 and h_2 the helicities of the fermion and antifermion. Then in the case of arbitrary polarizations of the initial particles and longitudinal polarizations of the final particles the differential cross section of the processes (2.1) can be represented in the form²⁷

$$\begin{aligned} \frac{d\sigma}{d\Omega} = & \frac{\alpha^2 N_c}{64} s \{ [|F_{LL}|^2 (1 - \lambda_1)(1 + \lambda_2)(1 - h_1)(1 + h_2) \\ & + |F_{RR}|^2 (1 + \lambda_1)(1 - \lambda_2)(1 + h_1)(1 - h_2)] \\ & \times (1 + \cos \theta)^2 + [|F_{LR}|^2 (1 - \lambda_1)(1 + \lambda_2)(1 + h_1) \\ & \times (1 - h_2) + |F_{RL}|^2 (1 + \lambda_1)(1 - \lambda_2)(1 - h_1) \\ & \times (1 + h_2)] (1 - \cos \theta)^2 - 2\eta_1 \eta_2 \sin^2 \theta [(1 - h_1) \\ & \times (1 + h_2) (\text{Re}(F_{LL} F_{RL}^*)) \cos 2\varphi \\ & + \text{Im}(F_{LL} F_{RL}^*) \sin 2\varphi + (1 + h_1)(1 - h_2) \\ & \times (\text{Re}(F_{LR} F_{RR}^*) \cos 2\varphi + \text{Im}(F_{LR} F_{RR}^*) \sin 2\varphi)] \}, \end{aligned} \quad (2.6)$$

where φ is the azimuthal angle of emission of the fermion f , measured from the plane of the transverse polarization of the initial leptons.

The effects of the superstring Z' boson are manifested in various characteristics, the expressions for which can be ob-

tained from the general expression (2.6) for the effective cross section. We first consider the differential characteristics of $e^-e^+ \rightarrow f\bar{f}$ processes.

Averaging over the polarization states of the electron and summing over the polarizations of the antifermion, we obtain for the differential cross section of the processes (2.1)

$$\frac{d\sigma}{d\cos\theta} = \frac{\pi d^2}{16} N_c s [|F_{LL}|^2 + |F_{LR}|^2 + |F_{RL}|^2 + |F_{RR}|^2] \times (1 + \cos^2\theta) [1 + A_{FB}(s, \theta)] \times [1 + \lambda_2 A_{RL}(s, \theta) + h_1 P(s, \theta)], \quad (2.7)$$

where $A_{FB}(s, \theta)$, $A_{RL}(s, \theta)$, and $P(s, \theta)$ are the forward-backward angular asymmetry, the right-left polarization asymmetry, and the degree of longitudinal polarization of the fermion. Measured experimentally, these differential characteristics are determined by the expressions

$$A_{FB}(s, \theta) = A_{FB}(s) f(\theta), \quad (2.8)$$

$$A_{RL}(s, \theta) = \frac{A_{RL}^{(1)}(s) + A_{RL}^{(2)}(s) f(\theta)}{1 + A_{FB}(s) f(\theta)}, \quad (2.9)$$

$$P(s, \theta) = \frac{P^{(1)}(s) + P^{(2)}(s) f(\theta)}{1 + A_{FB}(s) f(\theta)}. \quad (2.10)$$

Here

$$f(\theta) = 2 \cos\theta / (1 + \cos^2\theta),$$

$$A_{FB}(s) = \frac{|F_{LL}|^2 + |F_{RR}|^2 - |F_{LR}|^2 - |F_{RL}|^2}{|F_{LL}|^2 + |F_{LR}|^2 + |F_{RL}|^2 + |F_{RR}|^2}, \quad (2.11)$$

$$A_{RL}^{(1)}(s) = -P^{(2)}(s) \frac{|F_{LL}|^2 + |F_{LR}|^2 - |F_{RL}|^2 - |F_{RR}|^2}{|F_{LL}|^2 + |F_{LR}|^2 + |F_{RL}|^2 + |F_{RR}|^2}, \quad (2.12)$$

$$A_{RL}^{(2)}(s) = -P^{(1)}(s) \frac{|F_{LL}|^2 + |F_{RL}|^2 - |F_{RR}|^2 - |F_{LR}|^2}{|F_{LL}|^2 + |F_{LR}|^2 + |F_{RL}|^2 + |F_{RR}|^2}. \quad (2.13)$$

The experimental investigation of the angular and energy dependences of the asymmetries $A_{FB}(s, \theta)$ and $A_{RL}(s, \theta)$ and of the degree of longitudinal polarization $P(s, \theta)$ of the fermion can give valuable information about the chiral coupling constants of the fundamental fermions with the gauge bosons.

We consider the $\sqrt{s} = M_i$ regime, which can be studied at the LEP and SLC accelerators. In this case, the contribution to the cross section made by the gauge i boson ($i = Z$ or Z') becomes dominant. At resonance, the differential characteristics of the $e^-e^+ \rightarrow f\bar{f}$ processes have the form

$$A_{RL}^{(1)}(M_i^2) = -P^{(2)}(M_i^2) = \frac{(g_{Le}^i)^2 - (g_{Re}^i)^2}{(g_{Le}^i)^2 + (g_{Re}^i)^2} = A_e^i,$$

$$A_{RL}^{(2)}(M_i^2) = -P^{(1)}(M_i^2) = \frac{(g_{Lf}^i)^2 - (g_{Rf}^i)^2}{(g_{Lf}^i)^2 + (g_{Rf}^i)^2} = A_f^i,$$

$$A_{FB}(M_i^2) = A_e^i \cdot A_f^i. \quad (2.14)$$

It follows from this that the right-left asymmetry $A_{RL}^{(1)}(s)$ [or the degree of longitudinal polarization $P^{(2)}(s)$ of the

TABLE II. Polarization of the τ lepton as a function of the polar angle. The statistical errors are given.

Range of $\cos\theta$	Polarization	
	Experiment (Ref. 41)	Standard model ($x_w=0.232$)
$[-0.9; -0.7]$	-0.056 ± 0.053	-0.004
$[-0.7; -0.5]$	-0.026 ± 0.051	-0.017
$[-0.5; -0.3]$	-0.065 ± 0.056	-0.045
$[-0.3; -0.1]$	-0.056 ± 0.060	-0.088
$[-0.1; 0.1]$	-0.141 ± 0.063	-0.143
$[0.1; 0.3]$	-0.118 ± 0.059	-0.196
$[0.3; 0.5]$	-0.226 ± 0.054	-0.238
$[0.5; 0.7]$	-0.281 ± 0.050	-0.264
$[0.7; 0.9]$	-0.235 ± 0.050	-0.243

fermion] at the Z or Z' resonance does not depend on the nature of the produced particles and is determined solely by the electron coupling constants, whereas the asymmetry $A_{RL}^{(2)}(s)$ [or the degree of longitudinal polarization $P^{(1)}(s)$ of the fermion] is determined by the parameters of the weak neutral currents of the final particles.

The degree of longitudinal polarization of the τ lepton in the process $e^-e^+ \rightarrow \tau^- \tau^+$ at $s = M_Z^2$ has been measured at LEP by various collaborations (ALEPH, DELPHI, L3, OPAL).⁴⁰⁻⁴² The polarization of the τ lepton was measured using the spectrum of particles in the decays $\tau^- \rightarrow e^- \bar{\nu}_e \nu_\tau$, $\tau^- \rightarrow \mu^- \bar{\nu}_\mu \nu_\tau$, $\tau^- \rightarrow J_1^- \nu_\tau$, $\tau^- \rightarrow \rho^- \nu_\tau$.

At the Z resonance, the polarization (2.10) of the τ lepton takes the form

$$P(M_Z^2, \cos\theta) = -\frac{A_\tau^Z (1 + \cos^2\theta) + 2A_e^Z \cos\theta}{1 + \cos^2\theta + 2A_e^Z A_\tau^Z \cos\theta},$$

where

$$A_l^Z = [(g_{Ll}^Z)^2 - (g_{Rl}^Z)^2] / [(g_{Ll}^Z)^2 + (g_{Rl}^Z)^2] \quad (l = e, \tau).$$

In Table II, we give data on the measurement of the degree of longitudinal polarization of the τ lepton obtained by the ALEPH collaboration.⁴¹ We also give there the predictions of the standard model for the value $\sin^2\theta_w = 0.232$ of the Weinberg parameter. As can be seen from the table, within the errors the experimental data agree satisfactorily with the predictions of the standard model.

We now consider the integrated characteristics of $e^-e^+ \rightarrow f\bar{f}$ processes. The ones most frequently discussed are the following:

1) the forward-backward asymmetry in the case of unpolarized particles:

$$A_{FB} = \frac{\sigma_F - \sigma_B}{\sigma_F + \sigma_B} = \frac{3}{4} \cdot \frac{|F_{LL}|^2 + |F_{RR}|^2 - |F_{LR}|^2 - |F_{RL}|^2}{|F_{LL}|^2 + |F_{LR}|^2 + |F_{RL}|^2 + |F_{RR}|^2}, \quad (2.15)$$

where σ_F and σ_B are the cross sections for fermion production in the forward and backward hemispheres;

2) the right-left polarization asymmetry:

$$A_{RL} = \frac{\sigma_R - \sigma_L}{\sigma_R + \sigma_L} = \frac{|F_{LL}|^2 + |F_{LR}|^2 - |F_{RL}|^2 - |F_{RR}|^2}{|F_{LL}|^2 + |F_{LR}|^2 + |F_{RL}|^2 + |F_{RR}|^2}, \quad (2.16)$$

where σ_R and σ_L are the cross sections for annihilation of right- and left-polarized positrons;

3) the degree of longitudinal polarization of the fermion:

$$P = \frac{\sigma(f_R) - \sigma(f_L)}{\sigma(f_R) + \sigma(f_L)} = -\frac{|F_{LL}|^2 + |F_{RL}|^2 - |F_{LR}|^2 - |F_{RR}|^2}{|F_{LL}|^2 + |F_{RL}|^2 + |F_{LR}|^2 + |F_{RR}|^2}, \quad (2.17)$$

where $\sigma(f_R)$ and $\sigma(f_L)$ are the integrated cross sections for production of the fermion f in the final state with right and left polarization measured in the experiment.

It should be noted that in the standard model these integrated characteristics have vanishing values when the e^-e^+ beams have energies

$$\begin{aligned} s &= 2Q_f M_Z^2 (2Q_f - g_{Ve}^Z g_{Vf}^Z)^{-1}, \\ s &= 2Q_f M_Z^2 g_{Vf}^Z [2Q_f g_{Vf}^Z - g_{Ve}^Z ((g_{Lf}^Z)^2 + (g_{Rf}^Z)^2)]^{-1}, \\ s &= 2Q_f M_Z^2 g_{Ve}^Z [2Q_f g_{Ve}^Z - g_{Vf}^Z ((g_{Le}^Z)^2 + (g_{Re}^Z)^2)]^{-1}, \end{aligned}$$

respectively. In particular, if a $\mu^- \mu^+$ lepton pair is produced and we take the experimental value $\sin^2 \theta_W = 0.232$ (Ref. 41) of the Weinberg angle, then

$$\begin{aligned} A_{FB}^{(SM)} &= 0 \quad \text{at } \sqrt{s} = \sqrt{2} M_Z \sin 2\theta_W / \sqrt{1 + 8x_W^2} \approx M_Z, \\ A_{RL}^{(SM)} &= P^{(SM)} = 0 \quad \text{at } \sqrt{s} = \sqrt{2} M_Z \sin 2\theta_W / \sqrt{1 + 4x_W} \\ &= 0.86 M_Z. \end{aligned}$$

The forward-backward asymmetry of the angular distribution of the leptons in the reactions $e^-e^+ \rightarrow \mu^- \mu^+$ and $e^-e^+ \rightarrow \tau^- \tau^+$ was recently measured at LEP by various collaborations.³⁹⁻⁴² Figure 1 illustrates the energy dependence of the asymmetry A_{FB} in the standard model for Wein-

berg angle $\sin^2 \theta_W = 0.232$. Also given in Fig. 1 are the experimental data obtained by the ALEPH collaboration⁴¹ from measurement of the asymmetry A_{FB} in the $e^-e^+ \rightarrow \mu^- \mu^+$ and $e^-e^+ \rightarrow \tau^- \tau^+$ reactions. It can be seen that the forward-backward asymmetry vanishes at the point $\sqrt{s} = M_Z = 91.2$ GeV; this is also in agreement with the experimental results of Ref. 43, in which the mass of the Z boson was found with high accuracy: $M_Z = 91.187 \pm 0.007$ GeV.

In the case of annihilation of a transversely polarized e^-e^+ pair, the cross section (2.6) leads to the spin asymmetries

$$\begin{aligned} A_\varphi^{(1)} &= \frac{2}{\eta_1 \eta_2} \int_0^{2\pi} \cos 2\varphi d\varphi \int_{-1}^1 d \cos \theta \left(\frac{d\sigma}{d\Omega} \right) / \\ &\quad \int_0^{2\pi} d\varphi \int_{-1}^1 d \cos \theta \left(\frac{d\sigma}{d\Omega} \right) \\ &= \frac{-\text{Re}(F_{LL} F_{RL}^* + F_{LR} F_{RR}^*)}{|F_{LL}|^2 + |F_{RL}|^2 + |F_{LR}|^2 + |F_{RR}|^2}; \end{aligned} \quad (2.18)$$

$$\begin{aligned} A_\varphi^{(2)} &= \frac{2}{\eta_1 \eta_2} \int_0^{2\pi} \sin 2\varphi d\varphi \int_{-1}^1 d \cos \theta \left(\frac{d\sigma}{d\Omega} \right) / \\ &\quad \int_0^{2\pi} d\varphi \int_{-1}^1 d \cos \theta \left(\frac{d\sigma}{d\Omega} \right) \\ &= \frac{-\text{Im}(F_{LL}^{-1} F_{RL}^* + F_{LR} F_{RR}^*)}{|F_{LL}|^2 + |F_{RL}|^2 + |F_{LR}|^2 + |F_{RR}|^2}. \end{aligned} \quad (2.19)$$

In the standard model, the asymmetry $A_\varphi^{(1)}$ vanishes at two energies of the electron-positron beams:

$$s = \frac{M_Z^2 Q_f \{ 4Q_f - g_{Ve}^Z g_{Vf}^Z \pm ((g_{Ve}^Z)^2 (g_{Vf}^Z)^2 - 8g_{Le}^Z g_{Re}^Z ((g_{Lf}^Z)^2 + (g_{Rf}^Z)^2))^{1/2} \}}{2[2Q_f^2 - Q_f g_{Ve}^Z g_{Vf}^Z + g_{Le}^Z g_{Re}^Z ((g_{Lf}^Z)^2 + (g_{Rf}^Z)^2)]}.$$

In the $e^-e^+ \rightarrow \mu^- \mu^+ (\tau^- \tau^+)$ process,

$$A_\varphi^{(1)(SM)} = 0 \quad \text{at } \sqrt{s} = \begin{cases} \sqrt{2} M_Z \cos \theta_W \\ \sqrt{2} M_Z \sin 2\theta_W / \sqrt{1 + 4x_W} \end{cases}.$$

We now consider new characteristics—combined asymmetry coefficients.²⁰⁻²² These include the following:

1) the forward-backward asymmetry with allowance for the longitudinal polarization of the positron:

$$\begin{aligned} A_{FB}(\lambda_2) &= [\sigma_F(\lambda_2) - \sigma_B(\lambda_2)] / [\sigma_F(\lambda_2) + \sigma_B(\lambda_2)] \\ &= \frac{3(|F_{LL}|^2 - |F_{LR}|^2)(1 + \lambda_2) + (|F_{RR}|^2 - |F_{RL}|^2)(1 - \lambda_2)}{4(|F_{LL}|^2 + |F_{LR}|^2)(1 + \lambda_2) + (|F_{RR}|^2 + |F_{RL}|^2)(1 - \lambda_2)}; \end{aligned} \quad (2.20)$$

2) the forward polarization asymmetry:

$$\begin{aligned} A_F(\lambda_2) &= \frac{\sigma_F(\lambda_2) - \sigma_F(-\lambda_2)}{\sigma_F(\lambda_2) + \sigma_F(-\lambda_2)} \\ &= \lambda_2 \frac{7(|F_{LL}|^2 - |F_{RR}|^2) + |F_{LR}|^2 - |F_{RL}|^2}{7(|F_{LL}|^2 + |F_{RR}|^2) + |F_{LR}|^2 + |F_{RL}|^2}; \end{aligned} \quad (2.21)$$

3) the backward polarization asymmetry:

$$\begin{aligned} A_B(\lambda_2) &= \frac{\sigma_B(\lambda_2) - \sigma_B(-\lambda_2)}{\sigma_B(\lambda_2) + \sigma_B(-\lambda_2)} \\ &= \lambda_2 \frac{7(|F_{LR}|^2 - |F_{RL}|^2) + |F_{LL}|^2 - |F_{RR}|^2}{7(|F_{LR}|^2 + |F_{RL}|^2) + |F_{LL}|^2 + |F_{RR}|^2}; \end{aligned} \quad (2.22)$$

4) the forward-backward polarization asymmetry:

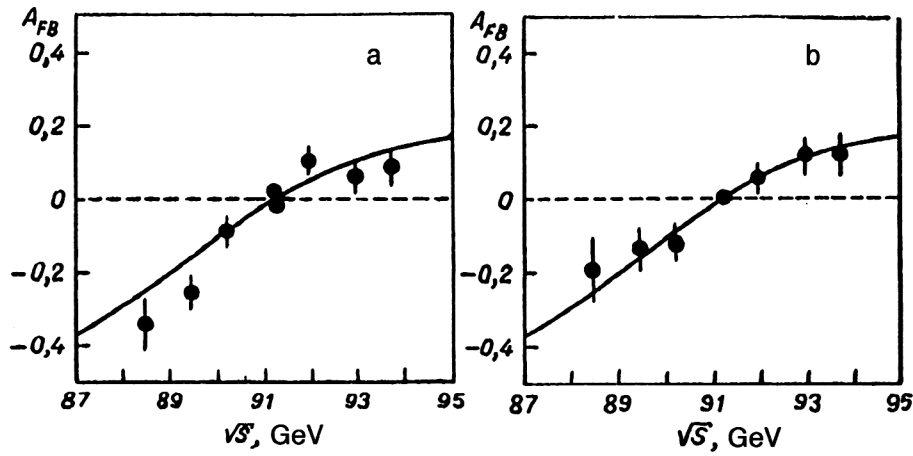


FIG. 1. Dependence of the asymmetry A_{FB} on the energy in the processes: a) $e^-e^+ \rightarrow \mu^-\mu^+$; b) $e^-e^+ \rightarrow \tau^-\tau^+$ for $\sin^2 \theta_W = 0.232$.

$$\begin{aligned}\tilde{A}_{FB}(\lambda_2) &= \frac{\sigma_F(\lambda_2) - \sigma_F(-\lambda_2) - [\sigma_B(\lambda_2) - \sigma_B(-\lambda_2)]}{\sigma_F(\lambda_2) + \sigma_F(-\lambda_2) + \sigma_B(\lambda_2) + \sigma_B(-\lambda_2)} \\ &= \frac{3}{4} \lambda_2 \cdot \frac{|F_{LL}|^2 + |F_{RL}|^2 - |F_{LR}|^2 - |F_{RR}|^2}{|F_{LL}|^2 + |F_{RL}|^2 + |F_{LR}|^2 + |F_{RR}|^2};\end{aligned}\quad (2.23)$$

5) the forward-backward asymmetry with allowance for the longitudinal polarization of the fermion:

$$\begin{aligned}A_{FB}(h_1) &= [\sigma_F(h_1) - \sigma_B(h_1)] / [\sigma_F(h_1) + \sigma_B(h_1)] \\ &= \frac{3}{4} \frac{(|F_{LL}|^2 - |F_{RL}|^2)(1 - h_1) + (|F_{RR}|^2 - |F_{LR}|^2)(1 + h_1)}{(|F_{LL}|^2 + |F_{RL}|^2)(1 - h_1) + (|F_{RR}|^2 + |F_{LR}|^2)(1 + h_1)};\end{aligned}\quad (2.24)$$

6) the forward asymmetry due to the polarization of the fermion:

$$\begin{aligned}A_F(h_1) &= \frac{\sigma_F(h_1) - \sigma_F(-h_1)}{\sigma_F(h_1) + \sigma_F(-h_1)} \\ &= h_1 \cdot \frac{7(|F_{RR}|^2 - |F_{LL}|^2) + |F_{LR}|^2 - |F_{RL}|^2}{7(|F_{RR}|^2 + |F_{LL}|^2) + |F_{LR}|^2 + |F_{RL}|^2};\end{aligned}\quad (2.25)$$

7) the backward asymmetry due to the polarization of the fermion:

$$\begin{aligned}A_B(h_1) &= \frac{\sigma_B(h_1) - \sigma_B(-h_1)}{\sigma_B(h_1) + \sigma_B(-h_1)} \\ &= h_1 \cdot \frac{7(|F_{LR}|^2 - |F_{RL}|^2) + |F_{RR}|^2 - |F_{LL}|^2}{7(|F_{LR}|^2 + |F_{RL}|^2) + |F_{RR}|^2 + |F_{LL}|^2};\end{aligned}\quad (2.26)$$

8) the forward-backward polarization asymmetry due to the polarization of the fermion:

$$\begin{aligned}\tilde{A}_{FB}(h_1) &= \frac{\sigma_F(h_1) - \sigma_F(-h_1) - [\sigma_B(h_1) - \sigma_B(-h_1)]}{\sigma_F(h_1) + \sigma_F(-h_1) + \sigma_B(h_1) + \sigma_B(-h_1)} \\ &= \frac{3}{4} h_1 \frac{|F_{RR}|^2 + |F_{RL}|^2 - |F_{LR}|^2 - |F_{LL}|^2}{|F_{RR}|^2 + |F_{RL}|^2 + |F_{LR}|^2 + |F_{LL}|^2}.\end{aligned}\quad (2.27)$$

In the standard model, the combined polarization asymmetries (2.20)–(2.27) also vanish at certain energies of the colliding e^-e^+ beams. For example,

$$\begin{aligned}A_{FB}^{(SM)}(\lambda_2 = 1) &= 0 \quad \text{at } s = 2Q_f M_Z^2 [2Q_f - g_{Le}^Z g_{\nu f}^Z]^{-1}, \\ A_{FB}^{(SM)}(\lambda_2 = -1) &= 0 \quad \text{at } s = 2Q_f M_Z^2 [2Q_f - g_{Re}^Z g_{\nu f}^Z]^{-1}, \\ A_{FB}^{(SM)}(h_1 = 1) &= 0 \quad \text{at } s = 2Q_f M_Z^2 [2Q_f - g_{Rf}^Z g_{\nu e}^Z]^{-1}, \\ A_{FB}^{(SM)}(h_1 = -1) &= 0 \quad \text{at } s = 2Q_f M_Z^2 [2Q_f - g_{Lf}^Z g_{\nu e}^Z]^{-1}.\end{aligned}$$

With regard to the forward and backward polarization asymmetries $A_F^{(SM)}(\lambda_2)$ and $A_B^{(SM)}(\lambda_2)$, they vanish at the energies

$$\begin{aligned}s &= 2Q_f M_Z^2 [7(g_{Le}^Z g_{Lf}^Z - g_{Re}^Z g_{Rf}^Z) + g_{Le}^Z g_{Rf}^Z - g_{Re}^Z g_{Lf}^Z] \\ &\quad \times \{2Q_f [7(g_{Le}^Z g_{Lf}^Z - g_{Re}^Z g_{Rf}^Z) + g_{Le}^Z g_{Rf}^Z - g_{Re}^Z g_{Lf}^Z] \\ &\quad - 7(g_{Le}^Z g_{Lf}^Z - g_{Re}^Z g_{Rf}^Z)(g_{Le}^Z g_{Lf}^Z + g_{Re}^Z g_{Rf}^Z) \\ &\quad + (g_{Re}^Z g_{Lf}^Z - g_{Le}^Z g_{Rf}^Z)(g_{Le}^Z g_{Rf}^Z + g_{Re}^Z g_{Lf}^Z)\}^{-1}\end{aligned}$$

and

$$\begin{aligned}s &= 2Q_f M_Z^2 [7(g_{Le}^Z g_{Rf}^Z - g_{Re}^Z g_{Lf}^Z) + g_{Le}^Z g_{Lf}^Z - g_{Re}^Z g_{Rf}^Z] \\ &\quad \times \{2Q_f [7(g_{Le}^Z g_{Rf}^Z - g_{Re}^Z g_{Lf}^Z) + g_{Le}^Z g_{Lf}^Z - g_{Re}^Z g_{Rf}^Z] \\ &\quad - 7(g_{Le}^Z g_{Rf}^Z - g_{Re}^Z g_{Lf}^Z)(g_{Le}^Z g_{Rf}^Z + g_{Re}^Z g_{Lf}^Z) \\ &\quad + (g_{Re}^Z g_{Rf}^Z - g_{Le}^Z g_{Lf}^Z)(g_{Re}^Z g_{Rf}^Z + g_{Le}^Z g_{Lf}^Z)\}^{-1},\end{aligned}$$

respectively. In particular, in the case of production of a lepton pair

TABLE III. Zeros of the helicity amplitudes and of the electroweak asymmetries of the processes $e^-e^+ \rightarrow f\bar{f}$.

Amplitude Asymmetry	Process		
	$e^-e^+ \rightarrow \mu^-\mu^+(\tau^+\tau^-)$	$e^-e^+ \rightarrow u\bar{u}(c\bar{c})$	$e^-e^+ \rightarrow d\bar{d}(s\bar{s}, b\bar{b})$
F_{RR}	$M_Z \cos \theta_W$	$M_Z \cos \theta_W$	$M_Z \cos \theta_W$
F_{LR}	$\sqrt{2}M_Z \cos \theta_W$	$\sqrt{2}M_Z \cos \theta_W$	$\sqrt{2}M_Z \cos \theta_W$
F_{RL}	$\sqrt{2}M_Z \cos \theta_W$	$2M_Z \cos \theta_W$	—
F_{LL}	$M_Z \sin 2\theta_W$	$\sqrt{2}M_Z \sin 2\theta_W / \sqrt{3-2x_W}$	$M_Z \sin 2\theta_W / \sqrt{3-4x_W}$
A_{FB}	$\sqrt{2}M_Z \sin 2\theta_W / \sqrt{1+8x_W^2}$	$2M_Z \sin 2\theta_W / \sqrt{3-4x_W+16x_W^2}$	$\sqrt{2}M_Z \sin 2\theta_W / \sqrt{3-8x_W(1-x_W)}$
A_{RL}	$\sqrt{2}M_Z \sin 2\theta_W / \sqrt{1+4x_W}$	$2M_Z \sin 2\theta_W \sqrt{1.5-4x_W} / \sqrt{4.5-6x_W-24x_W^2}$	$2M_Z \sin 2\theta_W \sqrt{1.5-2x_W} / \sqrt{9-24x_W}$
P	$\sqrt{2}M_Z \sin 2\theta_W / \sqrt{1+4x_W}$	$2M_Z \sin 2\theta_W \sqrt{0.5-2x_W} / \sqrt{1.5-2x_W-12x_W^2}$	$2M_Z \sin 2\theta_W \sqrt{0.5-2x_W} / \sqrt{3-8x_W}$
$A_{FB}(\lambda_2=1)$	$\sqrt{2}M_Z \sin 2\theta_W / \sqrt{1+2x_W}$	$2M_Z \sin 2\theta_W / \sqrt{3+2x_W}$	$\sqrt{2}M_Z \sin 2\theta_W / \sqrt{3-2x_W}$
$A_{FB}(\lambda_2=-1)$	$(2/\sqrt{3})M_Z \cos \theta_W$	$\sqrt{8/5}M_Z \cos \theta_W$	$2M_Z \cos \theta_W$
$A_{FB}(h_1=1)$	$(2/\sqrt{3})M_Z \cos \theta_W$	$(2/\sqrt{3})M_Z \cos \theta_W$	$(2/\sqrt{3})M_Z \cos \theta_W$
$A_{FB}(h_1=-1)$	$\sqrt{2}M_Z \sin 2\theta_W / \sqrt{1+2x_W}$	$(2/\sqrt{3})M_Z \sin 2\theta_W$	$\sqrt{2}M_Z \sin 2\theta_W / \sqrt{3(1-2x_W)}$

$$A_{F(B)}^{(SM)}(\lambda_2) = A_{F(B)}^{(SM)}(h_1) = 0$$

at

$$s = 2M_Z^2 [2 + (g_{Le}^Z)^2 + (g_{Re}^Z)^2]^{-1}.$$

Table III gives the zeros of the helicity amplitudes and of the electroweak asymmetries of the $e^-e^+ \rightarrow f\bar{f}$ processes.

To compare the results of the standard and E_6 superstring models with each other and also with the data of planned experiments, we have calculated the polarization characteristics of the $e^-e^+ \rightarrow f\bar{f}$ processes for Weinberg parameter $x_W=0.23$. It is clear that the Z - Z' mixing angle is $\Phi=0$, and for the mass and decay width of the additional boson we chose the values $M_{Z'}=150, 200, 250, 300$ GeV and $\Gamma_{Z'}=M_{Z'}/40$. Some numerical estimates of the electroweak asymmetries are given in Figs. 2 and 3. The dashed curves demonstrate the behavior of the electroweak asymmetries in the standard model.

The sensitivity of the asymmetries A_{FB} and A_{RL} to the

choice of the mass of the superstring Z' boson is illustrated by Fig. 2, which shows the dependence of the asymmetries on the energy \sqrt{s} . It can be seen that for $M_{Z'}=150$ GeV the asymmetry A_{FB} initially increases with increasing energy, then decreases, and, having reached a minimum value near $\sqrt{s} \sim 150$ GeV, again begins to increase to a maximum value. Further growth of the energy leads to a decrease of the asymmetry A_{FB} . An increase in the mass of the additional boson does not change the nature of the energy dependence of A_{FB} , but its maxima and minima are shifted to higher energies. A similar behavior is also observed for the other electroweak asymmetries.

We consider the $s=M_i^2$ regime of operation of e^-e^+ colliders. In this case, the contribution to the cross section from the i boson ($i=Z$ or Z') becomes dominant, since we are dealing with resonance production of the boson. At the resonance, the integrated characteristics of the $e^-e^+ \rightarrow f\bar{f}$ processes are

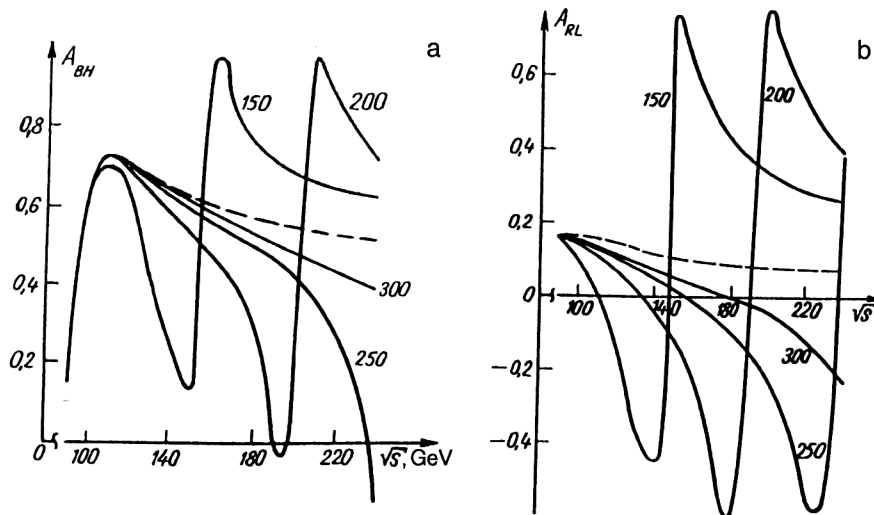


FIG. 2. Energy dependence of asymmetries: a) $A_{FB}(\theta_E=0^\circ)$; b) $A_{RL}(\theta_E=90^\circ)$ in the process $e^-e^+ \rightarrow \mu^-\mu^+$ for different masses of the Z' boson (the numbers next to the curves give the mass $M_{Z'}$, in giga-electron-volts).

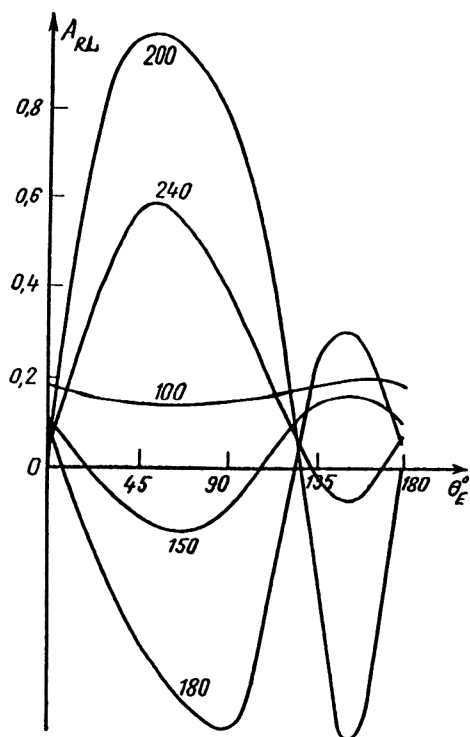


FIG. 3. Dependence of the right-left asymmetry on the angle θ_E in the process $e^-e^+ \rightarrow \mu^-\mu^+$ at different energies \sqrt{s} (the numbers next to the curves give the energy \sqrt{s} in giga-electron-volts).

$$\begin{aligned}
 A_{FB} &= \frac{3}{4} A_e^i A_f^i, \quad A_{RL} = A_e^i, \quad P = -A_f^i, \\
 A_F(\lambda_2) &= \lambda_2 \frac{4A_e^i + 3A_f^i}{4 + 3A_e^i A_f^i}, \quad A_B(\lambda_2) = \lambda_2 \frac{4A_e^i - 3A_f^i}{4 - 3A_e^i A_f^i}, \\
 A_{FB}(\lambda_2) &= \frac{3}{4} \frac{A_e^i + \lambda_2}{1 + \lambda_2 A_e^i} \cdot A_f^i, \quad \tilde{A}_{FB}(\lambda_2) = \frac{3}{4} \lambda_2 A_f^i, \\
 A_F(h_1) &= -h_1 \frac{4A_f^i + 3A_e^i}{4 + 3A_e^i A_f^i}, \\
 A_B(h_1) &= -h_1 \frac{4A_f^i - 3A_e^i}{4 - 3A_e^i A_f^i}, \\
 A_{FB}(h_1) &= \frac{3}{4} \frac{A_f^i - h_1}{1 - h_1 A_f^i} A_e^i,
 \end{aligned}$$

$$\tilde{A}_{FB}(h_1) = -\frac{3}{4} h_1 A_e^i,$$

$$A_\varphi^{(1)} = -g_{Le}^i g_{Re}^i / [(g_{Le}^i)^2 + (g_{Re}^i)^2].$$

Here

$$A_e^i = \frac{(g_{Le}^i)^2 - (g_{Re}^i)^2}{(g_{Le}^i)^2 + (g_{Re}^i)^2}, \quad A_f^i = \frac{(g_{Lf}^i)^2 - (g_{Rf}^i)^2}{(g_{Lf}^i)^2 + (g_{Rf}^i)^2}.$$

It follows from this that information about the constants of the coupling of the electron with the i bosons ($i=Z$ or Z') can be obtained by studying the asymmetries A_{RL} , $A_\varphi^{(1)}$, $\tilde{A}_{FB}(h_1)$, and $A_{FB}(h_1 = \pm 1)$. The degree of longitudinal polarization P of the fermion, the forward-backward asymmetry $A_{FB}(\lambda_2 = \pm 1)$, and the forward-backward polarization asymmetry $\tilde{A}_{FB}(\lambda_2)$ contain information about the parameters of the weak neutral currents of the final particles.

Table IV gives the values of the various electroweak asymmetries in the case of production of a pair of fundamental fermions in the Z and Z' resonance region of energies for the value $x_W = 0.23$ of the Weinberg parameter.

It is well known that in supersymmetric theories each fundamental fermion f is accompanied by a scalar fermion superpartner \tilde{f} . The scalar partners of the known fermions have the same quantum numbers as regards the internal symmetries and differ from them only in the spins. Intensive searches are being made for superparticles in various laboratories in the world, but as yet it has not been possible to discover them.

In electron-positron collisions, the $e^-e^+ \rightarrow \tilde{f}\tilde{f}^*$ annihilation process is the main source of production of scalar fermions. This reaction was investigated in Refs. 54–56 with allowance for the contribution of the weak neutral currents in the standard model. In particular, Bilenky and Nedelcheva⁵⁶ obtained general relations in the framework of $N=1$ supersymmetry between the polarization characteristics of $e^-e^+ \rightarrow \tilde{f}\tilde{f}^*$ processes.

There exist scalar fermions \tilde{f}_L and \tilde{f}_R that belong to supermultiplets (\tilde{f}_L, f_L) and (\tilde{f}_R, f_R) , where f_L and f_R are left and right fermions. Particles belonging to one supermultiplet have the same coupling constants with the gauge bosons.⁵⁷

To the process (2.2) of annihilation of an e^-e^+ pair into a pair of scalar fermions there correspond two helicity amplitudes:

$$M_A = \sum_{i=\gamma, Z_1, Z_2} D_i(s) g_{Ae}^i g_{Af}^i \quad (A=L, R), \quad (2.28)$$

TABLE IV. Electroweak asymmetries of $e^-e^+ \rightarrow f\bar{f}$ processes at the Z or Z' resonance for $\sin^2 \theta_W = 0.23$.

Fermion	Z resonance						
	A_{RL}	P	$A_F(\lambda_2)$	$A_B(\lambda_2)$	$A_{FB}(\lambda_2)$	$\tilde{A}_{FB}(\lambda_2)$	$A_\varphi^{(1)}$
μ, τ	0.16	-0.16	$0.28\lambda_2$	$0.04\lambda_2$	$0.12 (\lambda_2 + 0.16)/(1 + 0.16\lambda_2)$	$0.12\lambda_2$	0.5
u, c	0.16	-0.67	$0.61\lambda_2$	$-0.37\lambda_2$	$0.5 (\lambda_2 + 0.16)/(1 + 0.16\lambda_2)$	$0.5\lambda_2$	0.5
d, s, b	0.16	-0.94	$0.68\lambda_2$	$-0.6\lambda_2$	$0.7 (\lambda_2 + 0.16)/(1 + 0.16\lambda_2)$	$0.7\lambda_2$	0.5
$Z' = Z_x$ resonance ($\theta_E = 90^\circ$)							
μ, τ	0.8	-0.8	$0.95\lambda_2$	$0.4\lambda_2$	$0.6 (\lambda_2 + 0.8)/(1 + 0.8\lambda_2)$	$0.6\lambda_2$	-0.3
u, c	0.8	0	$0.8\lambda_2$	$0.8\lambda_2$	0	0	-0.3
d, s, b	0.8	0.8	$0.4\lambda_2$	$0.95\lambda_2$	$-0.6 (\lambda_2 + 0.8)/(1 + 0.8\lambda_2)$	$-0.6\lambda_2$	-0.3

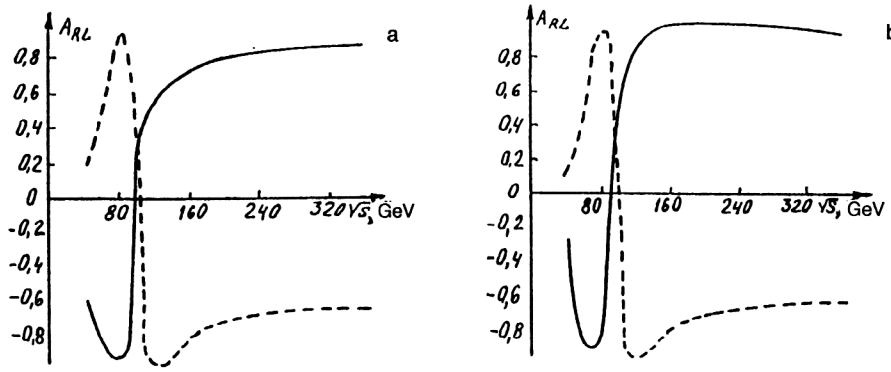


FIG. 4. Dependence of the asymmetry A_{RL} on the energy in the processes a) $e^-e^+ \rightarrow \tilde{u}\tilde{u}$; b) $e^-e^+ \rightarrow \tilde{d}\tilde{d}$.

which describe the reactions $e_L^- e_R^+ \rightarrow \tilde{f}\tilde{f}^*$ and $e_R^- e_L^+ \rightarrow \tilde{f}\tilde{f}^*$. Here $g_{\tilde{f}}^i$ are the coupling constants of the scalar fermion with the gauge i bosons, and for the superpartner \tilde{f}_L we have $g_{\tilde{f}}^i \equiv g_{\tilde{f}_L}^i$, and for \tilde{f}_R we have $g_{\tilde{f}}^i \equiv g_{\tilde{f}_R}^i$.

In the standard model, the helicity amplitudes of $e^-e^+ \rightarrow \tilde{f}\tilde{f}^*$ processes are given by

$$M_L^{(SM)} = \frac{Q_{\tilde{f}}}{s} + D_Z(s) g_{Le}^Z g_{\tilde{f}}^Z \quad (2.29)$$

$$M_R^{(SM)} = \frac{Q_{\tilde{f}}}{s} + D_Z(s) g_{Re}^Z g_{\tilde{f}}^Z. \quad (2.30)$$

The amplitudes $M_L^{(SM)}$ and $M_R^{(SM)}$ vanish at the energies

$$s = \frac{2M_Z^2 Q_{\tilde{f}} x_W (1-x_W)}{Q_{\tilde{f}} x_W - I_3^{\tilde{f}} (2x_W - 1)} \quad \text{and} \quad s = \frac{M_Z^2 Q_{\tilde{f}} (1-x_W)}{Q_{\tilde{f}} - I_3^{\tilde{f}}},$$

respectively. For a pair $\tilde{f}_R \tilde{f}_R^*$ of scalar fermions we have ($I_3^{\tilde{f}} = 0$)

$$M_L^{(SM)} = 0 \quad \text{at} \quad \sqrt{s} = \sqrt{2} M_Z \cos \theta_W,$$

$$M_R^{(SM)} = 0 \quad \text{at} \quad \sqrt{s} = M_Z \cos \theta_W,$$

irrespective of the nature of the scalar fermions.

The differential cross section of the $e^-e^+ \rightarrow \tilde{f}\tilde{f}^*$ reactions is^{25,27}

$$\frac{d\sigma}{d\Omega} = \frac{\alpha^2 \beta^3}{16} N_c s \sin^2 \theta [|M_L|^2 (1-\lambda_1)(1+\lambda_2) + |M_R|^2 (1+\lambda_1)(1-\lambda_2)]$$

$$- 2 \eta_1 \eta_2 [\text{Re}(M_L M_R^*) \cos 2\varphi + \text{Im}(M_L M_R^*) \sin 2\varphi] \}, \quad (2.31)$$

where β is the velocity of the scalar fermion.

The main integrated characteristics of the $e^-e^+ \rightarrow \tilde{f}\tilde{f}^*$ processes that are measured experimentally are the right-left polarization asymmetry

$$A_{RL} = [|M_L|^2 - |M_R|^2] / [|M_L|^2 + |M_R|^2], \quad (2.32)$$

the P -even transverse spin asymmetry

$$A_\varphi^{(1)} = -2 \text{Re}(M_L M_R^*) / [|M_L|^2 + |M_R|^2], \quad (2.33)$$

and the P -odd transverse spin asymmetry

$$A_\varphi^{(2)} = -2 \text{Im}(M_L M_R^*) / [|M_L|^2 + |M_R|^2]. \quad (2.34)$$

Figures 4 and 5 show the energy dependence of the right-left asymmetry A_{RL} and the transverse spin asymmetry $A_\varphi^{(1)}$ in the standard model for $x_W = 0.23$. In these figures, the solid curves correspond to $e^-e^+ \rightarrow \tilde{q}_L \tilde{q}_L^*$ processes, and the dashed curves to $e^-e^+ \rightarrow \tilde{q}_R \tilde{q}_R^*$ processes. For the scalar quarks $\tilde{q}_R \tilde{q}_R^*$ ($\tilde{q}_L \tilde{q}_L^*$) the right-left asymmetry A_{RL} increases (respectively, decreases) as the energy is increased and, having reached a maximum (minimum) at $\sqrt{s} \sim 80$ GeV, begins to decrease (respectively, increase) and vanishes at $\sqrt{s} \sim 93$ GeV ($\sqrt{s} \sim 90$ GeV), after which the asymmetry attains a minimum (maximum) and gradually enters a plateau regime.

A similar behavior is also observed for the P -even transverse spin asymmetry $A_\varphi^{(1)}$. Thus, at the beginning of the spectrum $A_\varphi^{(1)} = -1$; as the energy is increased, the asymme-

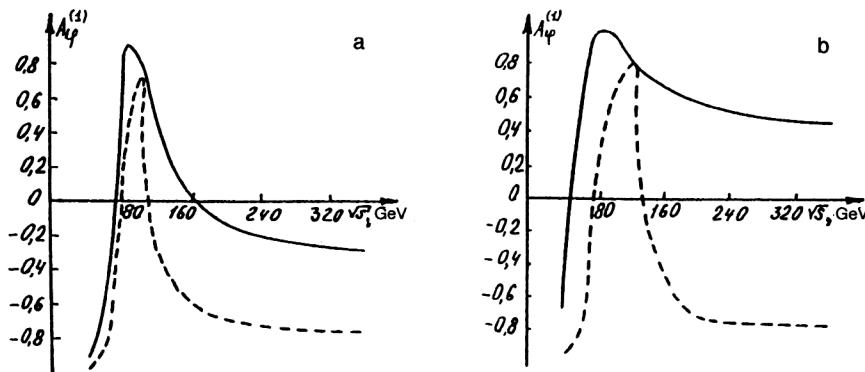


FIG. 5. Dependence of the asymmetry $A_\varphi^{(1)}$ on the energy in the processes a) $e^-e^+ \rightarrow \tilde{u}\tilde{u}$; b) $e^-e^+ \rightarrow \tilde{d}\tilde{d}$.

TABLE V. Zeros of the helicity amplitudes and of the asymmetries of the processes $e^-e^+ \rightarrow \tilde{f}\tilde{f}^*$

Process	Amplitude		Asymmetry	
	M_L	M_R	A_{RL}	$A_\phi^{(1)}$
$e^-e^+ \rightarrow \tilde{\mu}_R\tilde{\mu}_R^*$ $\tilde{\tau}_R\tilde{\tau}_R^*$	$\sqrt{2}M_Z \cos \theta_W$	$M_Z \cos \theta_W$	$(2/\sqrt{3})M_Z \cos \theta_W$	$M_Z \cos \theta_W$ $\sqrt{2}M_Z \cos \theta_W$
$e^-e^+ \rightarrow \tilde{\mu}_L\tilde{\mu}_L^*$ $\tilde{\tau}_L\tilde{\tau}_L^*$	$M_Z \sin 2\theta_W$	$\sqrt{2}M_Z \cos \theta_W$	$M_Z \sin 2\theta_W / \sqrt{0.5+x_W}$	$M_Z \sin 2\theta_W$ $\sqrt{2}M_Z \cos \theta_W$
$e^-e^+ \rightarrow \tilde{\mu}_R\tilde{u}_R^*$ $\tilde{c}_R\tilde{c}_R^*$	$\sqrt{2}M_Z \cos \theta_W$	$M_Z \cos \theta_W$	$(2/\sqrt{3})M_Z \cos \theta_W$	$\sqrt{2}M_Z \cos \theta_W$ $M_Z \cos \theta_W$
$e^-e^+ \rightarrow \tilde{u}_L\tilde{u}_L^*$ $\tilde{c}_L\tilde{c}_L^*$	$M_Z \sin 2\theta_W / \sqrt{1.5-x_W}$	$2M_Z \cos \theta_W$	$(2/\sqrt{3})M_Z \sin 2\theta_W$	$M_Z \sin 2\theta_W / \sqrt{1.5-x_W}$ $2M_Z \cos \theta_W$
$e^-e^+ \rightarrow \tilde{d}_R\tilde{d}_R^*$ $(\tilde{s}_R\tilde{s}_R, \tilde{b}_R\tilde{b}_R)$	$\sqrt{2}M_Z \cos \theta_W$	$M_Z \cos \theta_W$	$(2/\sqrt{3})M_Z \cos \theta_W$	$\sqrt{2}M_Z \cos \theta_W$ $M_Z \cos \theta_W$
$e^-e^+ \rightarrow \tilde{d}_L\tilde{d}_L^*$ $(\tilde{s}_L\tilde{s}_L, \tilde{b}_L\tilde{b}_L)$	$M_Z \sin 2\theta_W / \sqrt{3-4x_W}$	-	$M_Z \sin 2\theta_W / \sqrt{1.5-3x_W}$	$M_Z \sin 2\theta_W / \sqrt{3-4x_W}$

try increases and, having attained a maximum at $\sqrt{s} \sim 80-100$ GeV, begins to decrease. In $e^-e^+ \rightarrow \tilde{q}_R\tilde{q}_R^*$ processes, the asymmetry $A_\phi^{(1)}$ has two points at which it vanishes: at $\sqrt{s} \approx 80$ GeV and at $\sqrt{s} \approx 114$ GeV. For the scalar fermions $\tilde{u}_L\tilde{u}_L^*$, $\tilde{c}_L\tilde{c}_L^*$ ($\tilde{t}_L\tilde{t}_L^*$) the asymmetry $A_\phi^{(1)}$ also vanishes at two points: at $\sqrt{s} \approx 70$ GeV and at $\sqrt{s} \approx 160$ GeV; however, for the $e^-e^+ \rightarrow \tilde{d}_L\tilde{d}_L^*$, $\tilde{s}_L\tilde{s}_L^*$, $\tilde{b}_L\tilde{b}_L^*$ processes, a single point of vanishing is observed at $\sqrt{s} \approx 54$ GeV.

Table V gives the zeros of the helicity amplitudes and of the electroweak asymmetries of the $e^-e^+ \rightarrow \tilde{f}\tilde{f}^*$ processes in the standard model.

With regard to the P -odd transverse spin asymmetry $A_\phi^{(2)}$, it does not have points at which it vanishes: for the $e^-e^+ \rightarrow \tilde{f}_L\tilde{f}_L^*$ processes it is positive, and for the $e^-e^+ \rightarrow \tilde{f}_R\tilde{f}_R^*$ processes it is negative. This asymmetry initially increases in absolute magnitude with increasing energy, reaching the largest values in the region $\sqrt{s} \sim M_Z$, and it then decreases to zero.

The asymmetries A_{RL} and $A_\phi^{(1)}$ calculated in the framework of the E_6 superstring model, which at the start of the spectrum has approximately the same energy dependence, differs appreciably from the predictions of the standard model in the region of energies $\sqrt{s} \geq 100$ GeV, in which the asymmetries have additional zeros, a minimum, and a maximum.

3. HELICITY AMPLITUDES AND ELECTROWEAK ASYMMETRIES OF THE $e^-e^+ \rightarrow q\bar{q}g$ AND $e^-e^+ \rightarrow \tilde{q}\tilde{q}g$ PROCESSES

In $e^-e^+ \rightarrow X$ processes at high energies, hadrons are produced in the majority of events in the form of two jets. However, as the experiments show, in some cases additional jets are produced. In some studies (see the review of Ref. 48) there have been discussions of the mechanism of production of three jets in e^-e^+ annihilation through bremsstrahlung emission of a hard gluon leading to the production of a gluon jet.

Gluon jets must differ in several respects from quark jets. In the first place, the multiplicity of hadron production in a gluon jet must be greater than in a quark jet. This is due to the fact that a gluon can be transformed subsequently into

a quark-antiquark pair. Moreover, in a gluon jet η and η' mesons must be mainly produced. These properties make it possible to distinguish quark and gluon jets. In addition, it is possible to distinguish experimentally the hadron jets produced by quarks with different flavors. This is exceptionally important for determining the structure of the weak neutral currents of the heavy c , b , and, possibly, t quarks.

Three-jet annihilation of an e^-e^+ pair has been studied theoretically in the standard model by many authors.⁴⁹⁻⁵³ Here we consider the effects of a superstring Z' boson in processes of three-jet production of hadrons in the annihilation of an arbitrarily polarized electron-positron pair.

The production of a quark-antiquark pair with emission of a bremsstrahlung gluon in the electron-positron annihilation

$$e^- + e^+ \rightarrow (\gamma, Z_1, Z_2, \dots) \rightarrow q + \bar{q} + g \quad (3.1)$$

corresponds to the matrix element (the particle masses are ignored)

$$M = e^2 g_s \sum_i D_i(s) \bar{u} \gamma_\mu [g_{Le}^i (1 + \gamma_5) + g_{Re}^i (1 - \gamma_5)] u \bar{u}_\alpha \times \left(\frac{\lambda m}{2} \right)_{\alpha\beta} e_\rho^m \Gamma_{\mu\rho} [g_{Lq}^i (1 + \gamma_5) + g_{Rq}^i (1 - \gamma_5)] \vartheta_\beta, \quad (3.2)$$

where

$$\Gamma_{\mu\rho} = \gamma_\rho = \frac{\hat{q}_1 + \hat{k}}{2kq_1} \gamma_\mu - \gamma_\mu \frac{\hat{q}_2 + \hat{k}}{2kq_2} \gamma_\rho,$$

g_s is the quark-gluon coupling constant; q_1 , q_2 , and k are the 4-momenta of the quark, antiquark, and gluon; λ_m are the Gell-Mann matrices; $\alpha, \beta = 1, 2, 3$, and $m = 1-8$ are the color indices of the quark and gluon fields.

It follows from the expression (2) for the matrix element that to the process $e^-e^+ \rightarrow q\bar{q}g$ there correspond four helicity amplitudes F_{LL} , F_{LR} , F_{RL} , and F_{RR} , which describe the reactions

$$\begin{aligned} e_L^- + e_R^+ &\rightarrow q_L + \bar{q}_R + g, & e_L^- + e_R^+ &\rightarrow q_R + \bar{q}_L + g, \\ e_R^- + e_L^+ &\rightarrow q_L + \bar{q}_R + g, & e_R^- + e_L^+ &\rightarrow q_R + \bar{q}_L + g. \end{aligned}$$

In the E_6 superstring model, the helicity amplitudes of the $e^-e^+ \rightarrow q\bar{q}g$ process are determined by the same expressions as the amplitude of the $e^-e^+ \rightarrow q\bar{q}$ process:

$$F_{AB} = \sum_i D_i(s) g_{Ae}^i g_{Bq}^i \quad (A, B = L, R). \quad (3.3)$$

We write the expression for the square of the matrix element $|M|^2$ as

$$|M|^2 = (4\pi)^3 \alpha_s^2 N_c \sum_i \sum_k D_i(s) D_k^*(s) L_{\mu\nu}^{ik} H_{\mu\nu}^{ik}, \quad (3.4)$$

where $N_c=4$ is the color factor that takes into account the summation over the color degrees of freedom of the gluon and the quarks; $\alpha_s = g_s^2/4\pi$; $L_{\mu\nu}^{ik}$ and $H_{\mu\nu}^{ik}$ are the lepton and hadron tensors. Note that all the lepton and hadron tensors are conserved:

$$L_{\mu\nu}^{ik} q_\mu = L_{\mu\nu}^{ik} q_\nu = H_{\mu\nu}^{ik} q_\mu = H_{\mu\nu}^{ik} q_\nu = 0,$$

and, as a consequence of this, contributions to the cross section in the center-of-mass system, are made by only the spatial components of the tensors

$$L_{\mu\nu}^{ik} H_{\mu\nu}^{ik} = L_{mn}^{ik} H_{mn}^{ik} \quad (m, n = 1, 2, 3).$$

In the case of arbitrarily polarized e^-e^+ beams, the tensor L_{mn}^{ik} has the structure

$$\begin{aligned} L_{mn}^{ik} = & [(g_{Le}^i g_{Le}^k + g_{Re}^i g_{Re}^k)(1 - \lambda_1 \lambda_2) + (g_{Le}^i g_{Le}^k - g_{Re}^i g_{Re}^k) \\ & \times (\lambda_2 - \lambda_1)] L_{mn}^{(1)} + [(g_{Le}^i g_{Le}^k + g_{Re}^i g_{Re}^k)(\lambda_2 - \lambda_1) \\ & + (g_{Le}^i g_{Le}^k - g_{Re}^i g_{Re}^k)(1 - \lambda_2 \lambda_1)] L_{mn}^{(2)} + (g_{Le}^i g_{Re}^k \\ & + g_{Re}^i g_{Le}^k) L_{mn}^{(3)} + (g_{Re}^i g_{Le}^k - g_{Le}^i g_{Re}^k) L_{mn}^{(4)}, \end{aligned} \quad (3.5)$$

where

$$L_{mn}^{(1)} = s(\delta_{mn} - N_m N_n),$$

$$L_{mn}^{(2)} = i s \varepsilon_{mnr} N_r,$$

$$L_{mn}^{(3)} = s[\eta_{1m} \eta_{2n} + \eta_{1n} \eta_{2m} - \eta_1 \eta_2 (\delta_{mn} - N_m N_n)],$$

$$L_{mn}^{(4)} = i s (\eta_{1m} \varepsilon_{nrq} + \eta_{1n} \varepsilon_{mrq}) N_r \eta_{2q},$$

\mathbf{N} is the unit vector along the electron momentum; λ_1 and λ_2 (η_1 and η_2) are the longitudinal (respectively, transverse) polarizations of the electron and positron.

The expression for the hadron tensor H_{mn}^{ik} has the form

$$\begin{aligned} H_{mn}^{ik} = & [(g_{Lq}^i g_{Lq}^k + g_{Rq}^i g_{Rq}^k)(1 - h_1 h_2) + (g_{Lq}^i g_{Lq}^k \\ & - g_{Rq}^i g_{Rq}^k)(h_2 - h_1)] H_{mn}^{(s)} + [(g_{Lq}^i g_{Lq}^k + g_{Rq}^i g_{Rq}^k) \\ & \times (h_2 - h_1) + (g_{Lq}^i g_{Lq}^k - g_{Rq}^i g_{Rq}^k)(1 - h_1 h_2)] H_{mn}^{(a)}, \end{aligned} \quad (3.6)$$

where h_1 and h_2 are the quark and antiquark helicities, $H_{mn}^{(s)}$ and $H_{mn}^{(a)}$ are the symmetric and antisymmetric parts of the hadron tensor

$$\begin{aligned} H_{mn} = & \frac{1}{2(1-x_1)(1-x_2)} [\delta_{mn}(x_1^2 + x_2^2) - x_1^2 n_{1m} n_{1n} \\ & - x_2^2 n_{2m} n_{2n} + i \varepsilon_{mnr} (x_1^2 n_{1r} - x_2^2 n_{2r})], \end{aligned}$$

$x_1 = 2E_1/\sqrt{s}$ and $x_2 = 2E_2/\sqrt{s}$ are the energies of the quark and antiquark in units of the electron energy, and \mathbf{n}_1 and \mathbf{n}_2 are unit vectors along the momenta of the quark and antiquark.

We introduce the so-called correlation cross sections σ_a ($a=1, \dots, 9$) by means of the relations^{50,53}

$$\sigma_U = H_{11} + H_{22}, \quad \sigma_L = H_{33}, \quad \sigma_T = \frac{1}{2} (H_{22} - H_{11}),$$

$$\sigma_4 = -\frac{1}{2} (H_{12} + H_{21}), \quad \sigma_5 = -\frac{1}{2\sqrt{2}} (H_{23} + H_{32}),$$

$$\sigma_6 = -\frac{1}{2\sqrt{2}} (H_{31} + H_{13}), \quad \sigma_7 = i(H_{21} - H_{12}),$$

$$\sigma_8 = \frac{i}{2\sqrt{2}} (H_{32} - H_{23}), \quad \sigma_9 = \frac{i}{2\sqrt{2}} (H_{13} - H_{31}). \quad (3.7)$$

We have here introduced the special subscripts U, L, T for $a=1, 2, 3$. Expressions for the correlation cross sections σ_a are given in Appendix 1.

The tensor product $L_{mn}^{(k)} H_{mn}$ ($k=1, 2, 3, 4$) can be expressed in terms of the cross sections σ_a as

$$\begin{aligned} L_{mn}^{(k)} H_{mn} = & \frac{1}{2} (L_{11}^{(k)} + L_{22}^{(k)}) \sigma_U = L_{33}^{(k)} \sigma_L + (L_{22}^{(k)} - L_{11}^{(k)}) \sigma_T \\ & - (L_{21}^{(k)} + L_{12}^{(k)}) \sigma_4 - \sqrt{2} (L_{23}^{(k)} + L_{32}^{(k)}) \sigma_5 \\ & - \sqrt{2} (L_{13}^{(k)} + L_{31}^{(k)}) \sigma_6 + \frac{i}{2} (L_{12}^{(k)} - L_{21}^{(k)}) \sigma_7 \\ & + i\sqrt{2} (L_{23}^{(k)} - L_{32}^{(k)}) \sigma_8 + i\sqrt{2} (L_{31}^{(k)} - L_{13}^{(k)}) \sigma_9. \end{aligned} \quad (3.8)$$

We use a coordinate system in which the xz plane coincides with the plane of the events, $\mathbf{q}_1 + \mathbf{q}_2 + \mathbf{k} = 0$, and we introduce the angles θ, χ , and φ , where θ is the polar angle between the z axis and the direction of the electron beam, χ is the azimuthal angle between the plane of the events and the plane determined by the z axis and the e^- beam, and φ is the azimuthal angle between the plane of the events and the plane of the transverse polarization. Then the differential cross section of the processes (3.1) can be represented in the form

$$\begin{aligned} & \frac{d^5 \sigma}{d\varphi dx d \cos \theta dx_1 dx_2} \\ & = \frac{2\alpha^2}{3\pi^2} \alpha_s s \{ (\sigma_A + \sigma_D) [F_{LL}]^2 (1 - \lambda_2)(1 + \lambda_2)(1 - h_1) \} \end{aligned}$$

$$\begin{aligned}
& \times (1+h_2) \\
& + |F_{RR}|^2 (1+\lambda_1)(1-\lambda_2)(1+h_1)(1-h_2)] \\
& + (\sigma_A - \sigma_D) [|F_{LR}|^2 (1-\lambda_1)(1+\lambda_2)(1+h_1)(1-h_2) \\
& + |F_{RL}|^2 (1+\lambda_1)(1-\lambda_2)(1-h_1)(1+h_2)] - 2\eta_1\eta_2 \\
& \times [(1-h_1)(1+h_2)(\cos 2\varphi(\sigma_B \operatorname{Re}(F_{LL}F_{RL}^*) \\
& + \sigma_C \operatorname{Im}(F_{LL}F_{RL}^*)) + \sin 2\varphi(\sigma_B \operatorname{Im}(F_{LL}F_{RL}^*) \\
& - \sigma_C \operatorname{Re}(F_{LL}F_{RL}^*))) + (1+h_1)(1-h_2) \\
& \times (\cos 2\varphi(\sigma_B \operatorname{Re}(F_{LR}F_{RR}^*) + \sigma_C \operatorname{Im}(F_{LR}F_{RR}^*)) \\
& + \sin 2\varphi(\sigma_B \operatorname{Im}(F_{LR}F_{RR}^*) - \sigma_C \operatorname{Re}(F_{LR}F_{RR}^*)))]. \quad (3.9)
\end{aligned}$$

Here

$$\begin{aligned}
\sigma_A &= \frac{3}{8} (1 + \cos^2 \theta) \sigma_U + \frac{3}{4} \sin^2 \theta (\sigma_L + \cos 2\chi \sigma_T) \\
&\quad - \frac{3}{2\sqrt{2}} \sin 2\theta \cos \chi \sigma_I, \\
\sigma_B &= \frac{3}{8} \sin^2 \theta (\sigma_U - 2\sigma_L) + \frac{3}{4} (1 + \cos^2 \theta) \cos 2\chi \sigma_T \\
&\quad + \frac{3}{2\sqrt{2}} \sin 2\theta \cos \chi \sigma_I, \\
\sigma_C &= \frac{3}{2} \cos \theta \sin 2\chi \sigma_T + \frac{3}{\sqrt{2}} \sin \theta \sin \chi \sigma_I, \\
\sigma_D &= \frac{3}{4} \cos \theta \cdot \sigma_P - \frac{3}{\sqrt{2}} \sin \theta \cos \chi \sigma_F, \quad (3.10)
\end{aligned}$$

where we have adopted the notation $\sigma_I = \sigma_6$, $\sigma_P = \sigma_7$, $\sigma_F = \sigma_8$ and used the fact that $\sigma_4 = \sigma_5 = \sigma_9 = 0$ (see Appendix 1).

Correlation cross sections σ_a depend on the variables x_1 and x_2 ; they can be measured only if it is known from which parton a given jet of hadrons is produced, but this is difficult to determine experimentally. Therefore, the effective cross section of the processes (3.1) is expressed in terms of the measured quantity T , which is called the thrust, or elongation.

In the case of massless partons, the Dalitz plot is determined by the energy and momentum conservation laws:

$$x_1 + x_2 + x_3 = 2, \quad x_1 \mathbf{n}_1 + x_2 \mathbf{n}_2 + x_3 \mathbf{n}_3 = 0,$$

where $x_3 = 2w/\sqrt{s}$ is the gluon energy, and \mathbf{n}_1 , \mathbf{n}_2 , and \mathbf{n}_3 are unit vectors along the momenta of the partons. The boundaries of the allowed region are determined by the equations

$$x_k = |x_i \pm x_j| \quad (i \neq j \neq k).$$

The curves $x_1 = x_2$, $x_2 = x_3$, and $x_1 = x_3$ divide the Dalitz plot into six different regions. In region i_j , the parton energies satisfy the conditions

$$x_i \geq x_j \geq x_k \quad (i \neq j \neq k).$$

We denote by $T_1 = T = \max(x_1, x_2, x_3)$, T_2 , and T_3 the scaled energies of the most energetic, second most energetic, and least energetic jet: $T = T_1 \geq T_2 \geq T_3$. Choosing the z axis along the most energetic parton and integrating over T_2 (T_3 is expressed in terms of T and T_2 as $T_3 = 2 - T - T_2$) for fixed T in the different regions of the Dalitz diagram, we find the correlation energies σ_a as functions of the thrust.

The spectral and angular distribution of the most energetic quark jet is given by

$$\begin{aligned}
& \frac{d^4\sigma}{d\varphi d\chi d\cos\theta dT} \\
&= \frac{2}{3} \frac{\alpha^2}{\pi^2} \alpha_s \{ [|F_{LL}|^2 (1-\lambda_1)(1+\lambda_2)(1-h_1)(1+h_2) \\
&\quad + |F_{RR}|^2 (1+\lambda_1)(1+\lambda_2)(1+h_1)(1-h_2)] (\sigma_A + \sigma_D) \\
&\quad + (\sigma_A - \sigma_D) [|F_{LR}|^2 (1-\lambda_1)(1+\lambda_2)(1+h_1)(1-h_2) \\
&\quad + |F_{RL}|^2 (1+\lambda_1)(1-\lambda_2)(1-h_1)(1+h_2)] - 2\eta_1\eta_2 \\
&\quad \times [(1-h_1)(1+h_2)(\cos 2\varphi(\sigma_B \operatorname{Re}(F_{LL}F_{RL}^*) \\
&\quad + \sigma_C \operatorname{Im}(F_{LL}F_{RL}^*)) + \sin 2\varphi(\sigma_B \operatorname{Im}(F_{LL}F_{RL}^*) \\
&\quad - \sigma_C \operatorname{Re}(F_{LL}F_{RL}^*))) + (1+h_1)(1-h_2) \\
&\quad \times (\cos 2\varphi(\sigma_B \operatorname{Re}(F_{LR}F_{RR}^*) + \sigma_C \operatorname{Im}(F_{LR}F_{RR}^*)) \\
&\quad + \sin 2\varphi(\sigma_B \operatorname{Im}(F_{LR}F_{RR}^*) - \sigma_C \operatorname{Re}(F_{LR}F_{RR}^*))) \}. \quad (3.11)
\end{aligned}$$

where σ_A , σ_B , σ_C , and σ_D are determined by the previous expressions (3.10), but in them the correlation cross sections are

$$\begin{aligned}
\frac{d\sigma_U}{dT} &= \frac{1+T^2}{1-T} \ln \frac{2T-1}{1-T} - \frac{(3T-2)(2+2T-T^2)}{2T(1-T)}, \\
\frac{d\sigma_L}{dT} &= 2 \frac{d\sigma_T}{dT} = \frac{3T-2}{T}, \\
\frac{d\sigma_I}{dT} &= \frac{\sqrt{2(2T-1)}}{T} - \frac{1}{\sqrt{2(1-T)}}, \\
\frac{d\sigma_P}{dT} &= \frac{d\sigma_F}{dT} = \frac{1+T^2}{1-T} \ln \frac{2T-1}{1-T} \\
&\quad - \frac{(3T-2)(4-2T+T^2)}{2T(1-T)}. \quad (3.12)
\end{aligned}$$

We consider the distribution of the quark jet with respect to the angles θ and φ . Integrating the cross section (3.11) over the angles χ , we obtain

$$\begin{aligned}
& \frac{d^3\sigma}{d\varphi d \cos \theta dT} \\
&= \frac{\alpha^2}{\pi} \alpha_s s (\sigma_U + 2\sigma_L) \{ [|F_{LL}|^2(1-\lambda_1)(1+\lambda_2)(1-h_1) \\
&\quad \times (1+h_2) + |F_{RR}|^2(1+\lambda_1)(1-\lambda_2)(1+h_1)(1-h_2)] \\
&\quad \times [1 + \alpha(T) \cos^2 \theta + 2\beta(T) \cos \theta] \\
&\quad + [|F_{LR}|^2(1-\lambda_1)(1+\lambda_2)(1+h_1)(1-h_2) \\
&\quad + |F_{RL}|^2(1+\lambda_1)(1-\lambda_2)(1-h_1)(1+h_2)] \\
&\quad \times [1 + \alpha(T) \cos^2 \theta - 2\beta(T) \cos \theta] \\
&\quad - 2\eta_1 \eta_2 \sin^2 \theta [(1+h_1)(1-h_2) \\
&\quad \times (\cos 2\varphi \operatorname{Re}(F_{LR}F_{RR}^*) + \sin 2\varphi \operatorname{Im}(F_{LR}F_{RR}^*)) \\
&\quad + (1-h_1)(1+h_2)(\cos 2\varphi \operatorname{Re}(F_{LL}F_{RL}^*) \\
&\quad + \sin 2\varphi \operatorname{Im}(F_{LL}F_{RL}^*))]\}, \quad (3.13)
\end{aligned}$$

where

$$\alpha(T) = (\sigma_U - 2\sigma_L)/(\sigma_U + 2\sigma_L), \quad \beta(T) = \sigma_P/(\sigma_U + 2\sigma_L).$$

We define as follows the cross sections for production of a quark jet in the forward and backward hemispheres in the case of annihilation of a polarized positron and an unpolarized electron (there is a summation over the quark and anti-quark polarizations):

$$\sigma_F(\lambda_2) = \int_0^{2\pi} d\varphi \int_0^1 d \cos \theta \left(\frac{d^3\sigma}{d\varphi d \cos \theta dT} \right) \quad (3.14)$$

$$\sigma_B(\lambda_2) = \int_0^{2\pi} d\varphi \int_{-1}^0 d \cos \theta \left(\frac{d^3\sigma}{d\varphi d \cos \theta dT} \right). \quad (3.15)$$

Then on the basis of the expression (3.13),

$$\begin{aligned}
\sigma_{F(B)}(\lambda_2) &= \frac{8}{3} \alpha^2 \alpha_s s (\sigma_U + 2\sigma_L) \{ [|F_{LL}|^2(1+\lambda_2) \\
&\quad + |F_{RR}|^2(1-\lambda_2)][3 + \alpha(T) \pm 3\beta(T)] \\
&\quad + [|F_{LR}|^2(1+\lambda_2) + |F_{RL}|^2(1-\lambda_2)] \\
&\quad \times [3 + \alpha(T) \mp 3\beta(T)] \}. \quad (3.16)
\end{aligned}$$

This expression leads to the following integrated characteristics, which can be measured experimentally:

1) the forward-backward asymmetry in the case of unpolarized particles:

$$A_{FB} = \frac{\sigma_F - \sigma_B}{\sigma_F + \sigma_B} = \gamma(T) \frac{|F_{LL}|^2 + |F_{RR}|^2 - |F_{LR}|^2 - |F_{RL}|^2}{|F_{LL}|^2 + |F_{LR}|^2 + |F_{RL}|^2 + |F_{RR}|^2}, \quad (3.17)$$

where

$$\gamma(T) = 3\beta(T)/[3 + \alpha(T)] = \frac{3}{4} \sigma_P/(\sigma_U + \sigma_L);$$

2) the forward-backward asymmetry with allowance for longitudinal polarization of the positron:

$$\begin{aligned}
A_{FB}(\lambda_2) &= \frac{\sigma_F(\lambda_2) - \sigma_B(\lambda_2)}{\sigma_F(\lambda_2) + \sigma_B(\lambda_2)} = \gamma(T) \\
&\quad \times \frac{(|F_{LL}|^2 - |F_{LR}|^2)(1+\lambda_2) + (|F_{RR}|^2 - |F_{RL}|^2)(1-\lambda_2)}{(|F_{LL}|^2 + |F_{LR}|^2)(1+\lambda_2) + (|F_{RR}|^2 + |F_{RL}|^2)(1-\lambda_2)}, \quad (3.18)
\end{aligned}$$

3) the forward-backward polarization asymmetry:

$$\begin{aligned}
\tilde{A}_{FB}(\lambda_2) &= [\sigma_F(\lambda_2) - \sigma_F(-\lambda_2) - \sigma_B(\lambda_2) \\
&\quad + \sigma_B(-\lambda_2)]/[\sigma_F(\lambda_2) + \sigma_F(-\lambda_2) \\
&\quad + \sigma_B(\lambda_2) + \sigma_B(-\lambda_2)] \\
&= \lambda_2 \gamma(T) \frac{|F_{LL}|^2 + |F_{RL}|^2 - |F_{LR}|^2 - |F_{RR}|^2}{|F_{LL}|^2 + |F_{RR}|^2 + |F_{LR}|^2 + |F_{RL}|^2}; \quad (3.19)
\end{aligned}$$

4) the forward (respectively, backward) polarization asymmetry:

$$\begin{aligned}
A_{F(B)}(\lambda_2) &= [\sigma_{F(B)}(\lambda_2) - \sigma_{F(B)}(-\lambda_2)]/[\sigma_{F(B)}(\lambda_2) + \sigma_{F(B)}(-\lambda_2)] \\
&= \lambda_2 \frac{|F_{LL}|^2 + |F_{LR}|^2 - |F_{RL}|^2 - |F_{RR}|^2 \pm \gamma(T)[|F_{LL}|^2 + |F_{RL}|^2 - |F_{LR}|^2 - |F_{RR}|^2]}{|F_{LL}|^2 + |F_{RR}|^2 + |F_{LR}|^2 + |F_{RL}|^2 \pm \gamma(T)[|F_{LL}|^2 + |F_{RR}|^2 - |F_{LR}|^2 - |F_{RL}|^2]}, \quad (3.20)
\end{aligned}$$

5) the right-left polarization asymmetry:

$$A_{RL} = \frac{\sigma_R - \sigma_L}{\sigma_R + \sigma_L} = \frac{|F_{LL}|^2 + |F_{LR}|^2 - |F_{RL}|^2 - |F_{RR}|^2}{|F_{LL}|^2 + |F_{LR}|^2 + |F_{RL}|^2 + |F_{RR}|^2}, \quad (3.21)$$

where $\sigma_R = \sigma_F(\lambda_2=1) + \sigma_B(\lambda_2=1)$ and $\sigma_L = \sigma_F(\lambda_2=-1) + \sigma_B(\lambda_2=-1)$ are the cross sections for annihilation of right- and left-polarized positrons.

The integrated cross sections for the production of a longitudinally polarized quark jet in the case of annihilation of an unpolarized e^-e^+ pair are equal to

$$\begin{aligned}
\sigma_{F(B)}(h_1) &= \frac{4}{3} \alpha^2 \alpha_s s (\sigma_U + 2\sigma_L) \{ [|F_{LL}|^2(1-h_1) \\
&\quad + |F_{RR}|^2(1+h_1)][3 + \alpha(T) \pm 3\beta(T)] \\
&\quad + [|F_{LR}|^2(1+h_1) + |F_{RL}|^2(1-h_1)] \\
&\quad \times [3 + \alpha(T) \mp 3\beta(T)] \}. \quad (3.22)
\end{aligned}$$

From this the following P -odd electroweak asymmetries can be determined:

$$P = \frac{\sigma(h_1=1) - \sigma(h_1=-1)}{\sigma(h_1=1) + \sigma(h_1=-1)} = \frac{|F_{RR}|^2 + |F_{LR}|^2 - |F_{RL}|^2 - |F_{LL}|^2}{|F_{RR}|^2 + |F_{LR}|^2 + |F_{RL}|^2 + |F_{LL}|^2}, \quad (3.23)$$

where $\sigma(h_1) = \sigma_F(h_1) + \sigma_B(h_1)$;

$$A_{FB}(h_1) = \frac{\sigma_F(h_1) - \sigma_B(h_1)}{\sigma_F(h_1) + \sigma_B(h_1)} = \gamma(T)$$

$$\times \frac{(|F_{LL}|^2 - |F_{RL}|^2)(1 - h_1) + (|F_{RR}|^2 - |F_{LR}|^2)(1 + h_1)}{(|F_{LL}|^2 + |F_{RL}|^2)(1 - h_1) + (|F_{RR}|^2 + |F_{LR}|^2)(1 + h_1)}; \quad (3.24)$$

$$\begin{aligned} \tilde{A}_{FB}(h_1) &= [\sigma_F(h_1) - \sigma_F(-h_1) - \sigma_B(h_1) + \sigma_B(-h_1)] / \\ & \quad [\sigma_F(h_1) + \sigma_F(-h_1) + \sigma_B(h_1) + \sigma_B(-h_1)] \\ &= h_1 \gamma(T) \frac{|F_{RR}|^2 + |F_{RL}|^2 - |F_{LL}|^2 - |F_{LR}|^2}{|F_{LL}|^2 + |F_{RL}|^2 + |F_{LR}|^2 + |F_{RR}|^2}; \end{aligned} \quad (3.25)$$

$$\begin{aligned} A_{F(B)}(h_1) &= [\sigma_{F(B)}(h_1) - \sigma_{F(B)}(-h_1)] / [\sigma_{F(B)}(h_1) + \sigma_{F(B)}(-h_1)] \\ &= h_1 \frac{|F_{RR}|^2 + |F_{LR}|^2 - |F_{LL}|^2 - |F_{RL}|^2 \pm \gamma(T)[|F_{RR}|^2 + |F_{RL}|^2 - |F_{LL}|^2 - |F_{LR}|^2]}{|F_{LL}|^2 + |F_{LR}|^2 + |F_{RL}|^2 + |F_{RR}|^2 \pm \gamma(T)[|F_{LL}|^2 + |F_{RR}|^2 - |F_{LR}|^2 - |F_{RL}|^2]}. \end{aligned} \quad (3.26)$$

In the case of annihilation of a transversely polarized electron-positron pair, the cross section (13) leads to the spin asymmetries

$$\begin{aligned} A_\varphi^{(1)} &= \frac{2}{\eta_1 \eta_2} \int_0^{2\pi} \cos 2\varphi d\varphi \int_{-1}^1 d \cos \theta \left(\frac{d^3 \sigma}{d\varphi d \cos \theta dT} \right) / \\ & \quad \int_0^{2\pi} d\varphi \int_{-1}^1 d \cos \theta \left(\frac{d^3 \sigma}{d\varphi d \cos \theta dT} \right) = - \frac{\sigma_U - 2\sigma_L}{\sigma_U + \sigma_L} \\ & \quad \times \frac{\text{Re}(F_{LL}F_{RL}^* + F_{LR}F_{RR}^*)}{|F_{LL}|^2 + |F_{LR}|^2 + |F_{RL}|^2 + |F_{RR}|^2}; \end{aligned} \quad (3.27)$$

$$\begin{aligned} A_\varphi^{(2)} &= \frac{2}{\eta_1 \eta_2} \int_0^{2\pi} \sin 2\varphi d\varphi \int_{-1}^1 d \cos \theta \left(\frac{d^3 \sigma}{d\varphi d \cos \theta dT} \right) / \\ & \quad \int_0^{2\pi} d\varphi \int_{-1}^1 d \cos \theta \left(\frac{d^3 \sigma}{d\varphi d \cos \theta dT} \right) = - \frac{\sigma_U - 2\sigma_L}{\sigma_U + \sigma_L} \\ & \quad \times \frac{\text{Im}(F_{LL}F_{RL}^* + F_{LR}F_{RR}^*)}{|F_{LL}|^2 + |F_{LR}|^2 + |F_{RL}|^2 + |F_{RR}|^2}. \end{aligned} \quad (3.28)$$

Note that the helicity amplitudes and all the polarization characteristics of the $e^-e^+ \rightarrow q\bar{q}g$ processes considered above vanish in the standard model at certain energies of the colliding electron-positron beams. It is interesting that these zeros are observed at the same energies of the colliding e^-e^+ beams as for the reactions $e^-e^+ \rightarrow q\bar{q}$ of two-jet hadron production (see Table III).

The distribution of the antiquark jet with respect to the angles and the thrust is determined by the same expression (3.13) as for the quark jet, but it is necessary to make the substitutions $\sigma_P \rightarrow -\sigma_P$ and $\sigma_F \rightarrow -\sigma_F$ in it. With regard to the distribution of the gluon jet, the same expression remains valid, but now the correlation cross sections are

$$\frac{d\sigma_U}{dT} = \frac{2}{T} (2 - 2T + T^2) \left(\ln \frac{2T-1}{1-T} - \frac{3T-2}{T} \right),$$

$$\frac{d\sigma_L}{dT} = 2 \frac{d\sigma_T}{dT} = \frac{4(1-T)(3T-2)}{T^2},$$

$$\frac{d\sigma_I}{dT} = \sqrt{2} \frac{(1-T)(2-T)}{T^2} \left(2\sqrt{2T-1} - \frac{T}{\sqrt{1-T}} \right),$$

$$d\sigma_P/dT = d\sigma_F/dT = 0. \quad (3.29)$$

In the case of detection of a gluon jet, the fact that $\sigma_P = 0$ has the consequence that the asymmetries A_{FB} , $A_{FB}(\lambda_2)$, $\tilde{A}_{FB}(\lambda_2)$, $A_{FB}(h_1)$, and $\tilde{A}_{FB}(h_1)$ vanish, and therefore the presence of these asymmetries can be used to distinguish the quark (antiquark) and gluon jets.

In the supersymmetric extension of QCD, hadron jets can be produced not only by quarks and gluons but also by their supersymmetric scalar quark partners (\tilde{q}) and gluinos (\tilde{g}). Thus, in e^-e^+ annihilation it is possible to have not only the ordinary two- and three-jet production of hadrons, $e^-e^+ \rightarrow q\bar{q}$ and $e^-e^+ \rightarrow q\bar{q}g$, but also processes of production of supersymmetric jets obtained in the elementary subprocesses $e^-e^+ \rightarrow \tilde{q}\tilde{q}^*$, $e^-e^+ \rightarrow \tilde{q}\tilde{g}g$, $e^-e^+ \rightarrow \tilde{q}\tilde{q}\tilde{g}$, $e^-e^+ \rightarrow q\tilde{q}\tilde{g}$ (Refs. 53 and 58).

In the E_6 superstring model, the production of a pair of scalar quarks and a gluon in electron-positron annihilation,

$$e^- + e^+ \rightarrow (\gamma, Z_1, Z_2, \dots) \rightarrow \tilde{q} + \tilde{q}^* + g, \quad (3.30)$$

is described by the matrix element

$$M = e^2 \sum_i D_i(s) \bar{v} \gamma_\mu [g_{Le}^i(l + \gamma_5) + g_{Re}^i(1 - \gamma_5)] u \cdot J_\mu^i, \quad (3.31)$$

where

$$J_\mu^i = g_s \left(\frac{\lambda_m}{2} \right)_{\alpha\beta} e_\rho^m \left[\frac{2q_{1\rho}q_{2\mu}}{q_1 \cdot K} + \frac{2q_{2\rho}q_{1\mu}}{q_2 \cdot K} + 2\delta_{\rho\mu} \right] g_{\tilde{q}}^i,$$

q_1 , q_2 , and k are the 4-momenta of the scalar quark, antiquark, and gluon, respectively, $g_{\tilde{q}}^i$ are the constants of the weak neutral current of the scalar quark, and for \tilde{q}_L (\tilde{q}_R) we have $g_{\tilde{q}L}^i \equiv g_{Lq}^i$ (respectively, $g_{\tilde{q}R}^i \equiv g_{Rq}^i$).

To the $e^-e^+ \rightarrow \tilde{q}\tilde{q}g$ annihilation process there correspond two helicity amplitudes

$$M_A = \sum_i D_i(s) g_{Ae}^i g_{\tilde{q}}^i \quad (A=R,L), \quad (3.32)$$

which describe the reactions $e_R^-e_L^+ \rightarrow \tilde{q}\tilde{q}g$ and $e_L^-e_R^+ \rightarrow \tilde{q}\tilde{q}g$.

The differential cross section of the process (3.30) can be represented in the form

$$\begin{aligned} & \frac{d^5\sigma}{d\varphi d\chi d\cos\theta dx_1 dx_2} \\ &= \frac{4}{3} \frac{\alpha^2}{\pi^2} \alpha_s s \{ [|M_L|^2(1-\lambda_1)(1+\lambda_2) \\ &+ |M_R|^2(1+\lambda_1)(1-\lambda_2)] \sigma_A - 2\eta_1\eta_2 \\ &\times [\cos 2\varphi(\text{Re}(M_L M_R^*)\sigma_B + \text{Im}(M_L M_R^*)\sigma_C) \\ &+ \sin 2\varphi(\text{Im}(M_L M_R^*)\sigma_B - \text{Re}(M_L M_R^*)\sigma_C)] \}, \quad (3.33) \end{aligned}$$

where σ_A , σ_B , and σ_C are given by (3.10), and the expressions for the correlation cross sections σ_U , σ_L , σ_T , and σ_I are given in Appendix 2.

The distribution of the scalar quark (or scalar antiquark) jet in the process $e^-e^+ \rightarrow \tilde{q}\tilde{q}g$ with respect to the angles θ and φ and the thrust T is determined by

$$\begin{aligned} \frac{d^3\sigma}{d\varphi d\cos\theta dT} &= \frac{\alpha^2\alpha_s}{\pi} s(\sigma_U + 2\sigma_L) \\ &\times \{ [|M_L|^2(1-\lambda_1)(1+\lambda_2) \\ &+ |M_R|^2(1+\lambda_1)(1-\lambda_2)] [1 + \alpha(T)\cos^2\theta] \\ &- 2\eta_1\eta_2\alpha(T)\sin^2\theta [\text{Re}(M_L M_R^*)\cos 2\varphi \\ &+ \text{Im}(M_L M_R^*)\sin 2\varphi] \}, \quad (3.34) \end{aligned}$$

where

$$\alpha(T) = (\sigma_U - 2\sigma_L)/(\sigma_U + 2\sigma_L),$$

and the expressions for the correlation cross sections as functions of the thrust are given in Appendix 3.

The differential cross section (3.34) leads to the following asymmetries: the right-left polarization asymmetry

$$A_{RL} = [|M_L|^2 - |M_R|^2]/[|M_L|^2 + |M_R|^2], \quad (3.35)$$

the P -even transverse spin asymmetry

$$A_\varphi^{(1)} = \frac{\sigma_U - 2\sigma_L}{\sigma_U + \sigma_L} \text{Re}(M_L M_R^*) / [|M_L|^2 + |M_R|^2], \quad (3.36)$$

and the P -odd transverse spin asymmetry

$$A_\varphi^{(2)} = - \frac{\sigma_U - 2\sigma_L}{\sigma_U + \sigma_L} \text{Im}(M_L M_R^*) / [|M_L|^2 + |M_R|^2]. \quad (3.37)$$

The behavior of the asymmetries (35)–(37) is the same as in the processes of two-jet production $e^-e^+ \rightarrow \tilde{q}\tilde{q}$ of scalar quarks, the analysis of which was made in Sec. 2.

An important characteristic of the processes (3.30) is the distribution of the supersymmetric jets with respect to the angles θ and χ ; this follows from the expression (33):

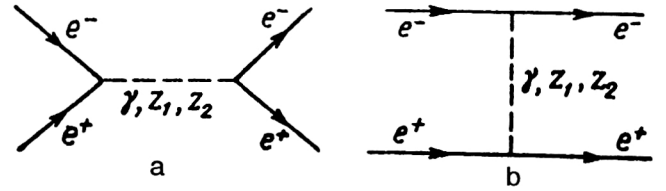


FIG. 6. Diagrams of the process $e^-e^+ \rightarrow (\gamma, Z_1, Z_2) \rightarrow e^-e^+$.

$$\begin{aligned} \frac{d^3\sigma}{d\chi d\cos\theta dT} &= \frac{\alpha^2\alpha_s}{\pi} s(\sigma_U + 2\sigma_L) [|M_L|^2(1-\lambda_1)(1 \\ &+ \lambda_2) + |M_R|^2(1+\lambda_1)(1-\lambda_2)] [1 \\ &+ \alpha(T)\cos^2\theta + \beta_1(T)\sin^2\theta \cos 2\chi \\ &+ \gamma_1(T)\sin 2\theta \cos \chi], \quad (3.38) \end{aligned}$$

where $\beta_1(T)$ and $\gamma_1(T)$ are the asymmetry parameters, which are determined by the correlation cross sections as

$$\beta_1(T) = 2\sigma_T/(\sigma_U + 2\sigma_L), \quad \gamma_1(T) = -2\sqrt{2}\sigma_I/(\sigma_U + 2\sigma_L).$$

Experimental study of the asymmetries A_{RL} , $A_\varphi^{(1)}$, and $A_\varphi^{(2)}$ and also of the asymmetry parameters $\alpha(T)$, $\beta_1(T)$, and $\gamma_1(T)$ opens up great prospects for thorough testing of the standard model of the electroweak interactions and for establishing the exact structure of the weak neutral currents at high energies.

4. HELICITY AMPLITUDES AND ELECTROWEAK ASYMMETRIES OF THE $e^-e^+ \rightarrow e^-e^+$ AND $e^-e^- \rightarrow e^-e^-$ PROCESSES

Among the most interesting electroweak processes are electron-positron and electron-electron scattering:

$$e^-e^+ \rightarrow (\gamma, Z_1, Z_2, \dots) \rightarrow e^-e^+, \quad (4.1)$$

$$e^-e^- \rightarrow (\gamma, Z_1, Z_2, \dots) \rightarrow e^-e^-, \quad (4.2)$$

which are being intensively investigated in experiments at the present time. Study of elastic electron-positron and electron-electron scattering at the high energies at which the contribution of the additional hypothetical Z' boson becomes significant may be the next stage in testing theoretical ideas about the weak interactions of leptons.

In the E_6 superstring model, the elastic electron-positron scattering (4.1) is described by the s - and t -channel diagrams given in Figs. 6a and 6b.

The annihilation diagrams correspond to four independent helicity amplitudes, which describe the processes

$$e_L^-e_R^+ \rightarrow e_L^-e_R^+, \quad e_L^-e_R^+ \rightarrow e_R^-e_L^+,$$

$$e_R^-e_L^+ \rightarrow e_L^-e_R^+, \quad e_R^-e_L^+ \rightarrow e_R^-e_L^+.$$

The differential cross sections corresponding to these four processes are²³

$$\begin{aligned}
\frac{d\sigma}{d\Omega} (e_L^- e_R^+ \rightarrow e_L^- e_R^+) &= \frac{\alpha^2}{s} u^2 |F_{LL}(s)|^2, \\
\frac{d\sigma}{d\Omega} (e_L^- e_R^+ \rightarrow e_R^- e_L^+) &= \frac{\alpha^2}{s} t^2 |F_{LR}(s)|^2, \\
\frac{d\sigma}{d\Omega} (e_R^- e_L^+ \rightarrow e_L^- e_R^+) &= \frac{\alpha^2}{s} t^2 |F_{RL}(s)|^2, \\
\frac{d\sigma}{d\Omega} (e_R^- e_L^+ \rightarrow e_R^- e_L^+) &= \frac{\alpha^2}{s} u^2 |F_{RR}(s)|^2.
\end{aligned} \quad (4.3)$$

Here

$$F_{AB}(s) = \sum_{i=\gamma, Z_1, Z_2} D_i(s) g_{Ae}^i g_{Be}^i \quad (A, B=L, R) \quad (4.4)$$

are the s -channel helicity amplitudes;

$$u = (s/2)(1 + \cos \theta), \quad t = (s/2)(1 - \cos \theta)$$

are the kinematic variables; $D_i(s)$ is the propagator of the vector i boson; and θ is the electron scattering angle.

The conservation of the fermion helicity at high energies has the consequence that for the t -channel diagrams too, there can be only four independent helicity amplitudes, which describe the processes

$$\begin{aligned}
e_L^- + e_R^+ \rightarrow e_L^- + e_R^+, \quad e_L^- + e_L^+ \rightarrow e_L^- + e_L^+, \\
e_R^- + e_L^+ \rightarrow e_R^- + e_L^+, \quad e_R^- + e_R^+ \rightarrow e_R^- + e_R^+.
\end{aligned}$$

These processes correspond to the differential cross sections

$$\begin{aligned}
\frac{d\sigma}{d\Omega} (e_L^- e_R^+ \rightarrow e_L^- e_R^+) &= \frac{\alpha^2}{s} u^2 |F_{LL}(t)|^2, \\
\frac{d\sigma}{d\Omega} (e_L^- e_L^+ \rightarrow e_L^- e_L^+) &= \alpha^2 s |F_{LR}(t)|^2, \\
\frac{d\sigma}{d\Omega} (e_R^- e_L^+ \rightarrow e_R^- e_L^+) &= \frac{\alpha^2}{s} u^2 |F_{RR}(t)|^2, \\
\frac{d\sigma}{d\Omega} (e_R^- e_R^+ \rightarrow e_R^- e_R^+) &= \alpha^2 s |F_{RL}(t)|^2.
\end{aligned} \quad (4.5)$$

Here

$$F_{AB}(t) = \sum_{i=\gamma, Z_1, Z_2} D_i(t) g_{Ae}^i g_{Be}^i \quad (A, B=L, R) \quad (4.6)$$

are the t -channel helicity amplitudes.

Among the four s -channel and four t -channel helicity amplitudes there is interference between only the two amplitudes describing the processes

$$e_L^- + e_R^+ \rightarrow e_L^- + e_R^+, \quad e_R^- + e_L^+ \rightarrow e_R^- + e_L^+.$$

Thus, the process of elastic electron-positron scattering is characterized by just six independent helicity amplitudes, which describe the processes

$$\begin{aligned}
1) \quad e_L^- e_R^+ \rightarrow e_L^- + e_R^+, \quad 2) \quad e_R^- + e_L^+ \rightarrow e_R^- + e_L^+, \\
3) \quad e_L^- + e_L^+ \rightarrow e_L^- + e_L^+, \quad 4) \quad e_R^- + e_R^+ \rightarrow e_R^- + e_R^+,
\end{aligned}$$

$$5) \quad e_L^- + e_R^+ \rightarrow e_R^- + e_L^+, \quad 6) \quad e_R^- + e_L^+ \rightarrow e_L^- + e_R^+.$$

The differential cross sections corresponding to these processes are

$$\begin{aligned}
\frac{d\sigma}{d\Omega} (e_L^- e_R^+ \rightarrow e_L^- e_R^+) &= \frac{\alpha^2}{s} u^2 |F_{LL}(s, t)|^2, \\
\frac{d\sigma}{d\Omega} (e_R^- e_L^+ \rightarrow e_R^- e_L^+) &= \frac{\alpha^2}{s} u^2 |F_{RR}(s, t)|^2, \\
\frac{d\sigma}{d\Omega} (e_L^- e_L^+ \rightarrow e_L^- e_L^+) &= \alpha^2 s |F_{LR}(t)|^2, \\
\frac{d\sigma}{d\Omega} (e_R^- e_R^+ \rightarrow e_R^- e_R^+) &= \alpha^2 s |F_{RL}(t)|^2, \\
\frac{d\sigma}{d\Omega} (e_L^- e_R^+ \rightarrow e_R^- e_L^+) &= \frac{\alpha^2}{s} t^2 |F_{LR}(s)|^2, \\
\frac{d\sigma}{d\Omega} (e_R^- e_L^+ \rightarrow e_L^- e_R^+) &= \frac{\alpha^2}{s} t^2 |F_{RL}(s)|^2.
\end{aligned} \quad (4.7)$$

We have here introduced the notation

$$F_{LL}(s, t) = F_{LL}(s) + F_{LL}(t), \quad F_{RR}(s, t) = F_{RR}(s) + F_{RR}(t).$$

In the standard model, the helicity amplitudes $F_{LR}(s)$ and $F_{RL}(s)$ describing the processes $e_L^- e_R^+ \rightarrow e_R^- e_L^+$ and $e_R^- e_L^+ \rightarrow e_L^- e_R^+$ have zeros at the energy $\sqrt{s} = \sqrt{2} M_Z \cos \theta_W$ of the colliding $e^- e^+$ beams. In this connection, it is highly desirable to have a thorough investigation of this process in the case of polarized $e^- e^+$ beams.

Experiments on $e^- e^+$ scattering with longitudinally polarized beams near the considered energies can be regarded as an alternative test of the standard model and also as a method of investigating new physics.

If the polarization of the final particles is not measured, the process of elastic electron-positron scattering is characterized by the four amplitudes

$$\begin{aligned}
\frac{d\sigma}{d\Omega} (e_L^- e_R^+ \rightarrow e^- e^+) &= \frac{\alpha^2}{s} [u^2 |F_{LL}(s, t)|^2 + t^2 |F_{LR}(s)|^2], \\
\frac{d\sigma}{d\Omega} (e_R^- e_L^+ \rightarrow e^- e^+) &+ \frac{\alpha^2}{s} [u^2 |F_{RR}(s, t)|^2 + t^2 |F_{RL}(s)|^2], \\
\frac{d\sigma}{d\Omega} (e_L^- e_L^+ \rightarrow e^- e^+) &= \alpha^2 s |F_{LR}(t)|^2, \\
\frac{d\sigma}{d\Omega} (e_R^- e_R^+ \rightarrow e^- e^+) &+ \alpha^2 s |F_{RL}(t)|^2.
\end{aligned} \quad (4.8)$$

We denote by λ_1 and h_1 (λ_2 and h_2) the helicities of the initial and final electrons (respectively, positrons). Then the differential cross section of the process $e^- e^+ \rightarrow e^- e^+$ can be represented in the form²³

$$\begin{aligned}
\frac{d\sigma}{d\Omega} &= \frac{\alpha^2}{16s} \{ u^2 [|F_{LL}(s, t)|^2 (1 - \lambda_1)(1 + \lambda_2)(1 - h_1)(1 + h_2) \\
&+ |F_{RR}(s, t)|^2 (1 + \lambda_1)(1 - \lambda_2)(1 + h_1)(1 - h_2)] \\
&+ s^2 |F_{LR}(t)|^2 [(1 - \lambda_1)(1 - \lambda_2)(1 - h_1)(1 - h_2)] \}
\end{aligned}$$

$$\begin{aligned}
& + (1 + \lambda_1)(1 + \lambda_2)(1 + h_1)(1 + h_2)] + t^2 |F_{LR}(s)|^2 \\
& \times [(1 - \lambda_1)(1 + \lambda_2)(1 + h_1)(1 - h_2) \\
& + (1 + \lambda_1)(1 - \lambda_2)(1 - h_1)(1 + h_2)] \}. \quad (4.9)
\end{aligned}$$

Effects of the superstring Z' boson are manifested in the various characteristics of the process $e^- e^+ \rightarrow e^- e^+$, expressions for which can be obtained from the general result (4.9) for the effective cross section. Among these characteristics, particular interest attaches to the P -odd right-left asymmetry A_{RL} , which is defined as

$$A_{RL} = (d\sigma_R - d\sigma_L) / (d\sigma_R + d\sigma_L) = B_4 / (B_1 + B_2 + B_3), \quad (4.10)$$

where

$$B_1 = 2s^2 |F_{LR}(t)|^2, \quad B_2 = 2t^2 |F_{LR}(s)|^2,$$

$$\tilde{A}_{\lambda_1 \lambda_2} = \frac{1}{\lambda_1 \lambda_2} \frac{d\sigma(\lambda_1, \lambda_2) - d\sigma(-\lambda_1, \lambda_2) - d\sigma(\lambda_1, -\lambda_2) + d\sigma(-\lambda_1, -\lambda_2)}{d\sigma(\lambda_1, \lambda_2) + d\sigma(-\lambda_1, \lambda_2) + d\sigma(\lambda_1, -\lambda_2) + d\sigma(-\lambda_1, -\lambda_2)} = (B_1 - B_2 - B_3) / (B_1 + B_2 + B_3), \quad (4.13)$$

$$N_\lambda = \frac{d\sigma(\lambda_1) - d\sigma(\lambda_1 = 0)}{d\sigma(\lambda_1) + d\sigma(\lambda_1 = 0)} = \frac{\lambda_1 B_4}{2(B_1 + B_2 + B_3) + \lambda_1 B_4}, \quad (4.14)$$

$$P = \frac{d\sigma(h_1 = 1) - d\sigma(h_1 = -1)}{d\sigma(h_1 = 1) + d\sigma(h_1 = -1)} = A_{RL}, \quad (4.15)$$

$P(\lambda_1, \lambda_2)$

$$\begin{aligned}
& = \frac{d\sigma(\lambda_1, \lambda_2, h_1 = 1) - d\sigma(\lambda_1, \lambda_2, h_1 = -1)}{d\sigma(\lambda_1, \lambda_2, h_1 = 1) + d\sigma(\lambda_1, \lambda_2, h_1 = -1)} \\
& = \frac{B_1(\lambda_1 + \lambda_2) + (B_3 - B_2)(\lambda_1 - \lambda_2) + B_4(1 - \lambda_1 \lambda_2)}{B_1(1 + \lambda_1 \lambda_2) + (B_2 + B_3)(1 - \lambda_1 \lambda_2) + B_4(\lambda_1 - \lambda_2)}. \quad (4.16)
\end{aligned}$$

Note that if the spins of the electron and positron before the scattering are antiparallel ($\lambda_1 = \lambda_2 = \pm 1$), then, as follows from (4.16), the scattered electrons remain completely longitudinally polarized: $P(\lambda_1 = \lambda_2 = \pm 1) = (\lambda_1 + \lambda_2) / (1 + \lambda_1 \lambda_2) = \pm 1$.

The same result was obtained in Ref. 59 through the electromagnetic mechanism of electron-positron scattering.

In the case of transverse polarizations of the initial particles, the differential cross section of the process (4.1) has the form (summation over the polarizations of the final particles)

$$\frac{d\sigma}{d\Omega} = \frac{\alpha^2}{4s} [B_1 + B_2 + B_3 + \eta_1 \eta_2 (B_5 \cos 2\varphi + B_6 \sin 2\varphi)], \quad (4.17)$$

where

$$B_{3(4)} = u^2 [|F_{RR}(s, t)|^2 \pm |F_{LL}(s, t)|^2],$$

and $d\sigma_R$ and $d\sigma_L$ are the cross sections for scattering of right- and left-polarized electrons by an unpolarized positron.

To establish the effects of the superstring Z' boson, we consider in addition to the right-left asymmetry A_{RL} the following polarization characteristics of the process (4.1):

$$A_{\lambda_1} = \frac{1}{\lambda_1} \cdot \frac{d\sigma(\lambda_1) - d\sigma(-\lambda_1)}{d\sigma(\lambda_1) + d\sigma(-\lambda_1)} = -A_{\lambda_2} = A_{RL}, \quad (4.11)$$

$$\begin{aligned}
A_{\lambda_1 \lambda_2} & = \frac{d\sigma(\lambda_1, \lambda_2) - d\sigma(-\lambda_1, -\lambda_2)}{d\sigma(\lambda_1, \lambda_2) + d\sigma(-\lambda_1, -\lambda_2)} \\
& = \frac{(\lambda_1 - \lambda_2) B_4}{B_1(1 + \lambda_1 \lambda_2) + (B_2 + B_3)(1 - \lambda_1 \lambda_2)}, \quad (4.12)
\end{aligned}$$

$$\begin{aligned}
B_5 & = -2ut [\operatorname{Re}(F_{LL}(s) F_{RL}^*(s)) + \operatorname{Re}(F_{LR}(s) F_{RR}^*(s)) \\
& \quad + \operatorname{Re}(F_{LR}(s) (F_{LL}^*(t) + F_{RR}^*(t)))],
\end{aligned}$$

$$\begin{aligned}
B_6 & = -2ut [\operatorname{Im}(F_{LL}(s) F_{RL}^*(s)) + \operatorname{Im}(F_{LR}(s) F_{RR}^*(s)) \\
& \quad + \operatorname{Im}(F_{LR}(s) (F_{LL}^*(t) - F_{RR}^*(t)))],
\end{aligned}$$

φ is the azimuthal angle of electron emission, and η_1 and η_2 are the transverse polarizations of the electron and positron.

From (4.17), we can determine the transverse spin asymmetries, which can be measured experimentally:

$$\begin{aligned}
A_\varphi^{(1)} & = \frac{2}{\eta_1 \eta_2} \int_0^{2\pi} \cos 2\varphi d\varphi \left(\frac{d\sigma}{d\Omega} \right) / \int_0^{2\pi} d\varphi \left(\frac{d\sigma}{d\Omega} \right) \\
& = \frac{B_5}{B_1 + B_2 + B_3}, \quad (4.18)
\end{aligned}$$

$$\begin{aligned}
A_\varphi^{(2)} & = \frac{2}{\eta_1 \eta_2} \int_0^{2\pi} \sin 2\varphi d\varphi \left(\frac{d\sigma}{d\Omega} \right) / \int_0^{2\pi} d\varphi \left(\frac{d\sigma}{d\Omega} \right) \\
& = \frac{B_6}{B_1 + B_2 + B_3}. \quad (4.19)
\end{aligned}$$

We now consider the elastic electron-electron scattering (4.2). As in the case of elastic electron-positron scattering, the $e^- e^- \rightarrow e^- e^-$ reactions correspond to just six helicity amplitudes, which describe the processes

- 1) $e_L^- + e_L^- \rightarrow e_L^- + e_L^-$, 2) $e_R^- + e_R^- \rightarrow e_R^- + e_R^-$,
- 3) $e_L^- + e_R^- \rightarrow e_L^- + e_R^-$, 4) $e_R^- + e_L^- \rightarrow e_R^- + e_L^-$,
- 5) $e_L^- + e_R^- \rightarrow e_R^- + e_L^-$, 6) $e_R^- + e_L^- \rightarrow e_L^- + e_R^-$.

These processes correspond to the differential cross sections

$$\begin{aligned}
\frac{d\sigma}{d\Omega} (e_L^- e_L^- \rightarrow e_L^- e_L^-) &= \alpha^2 s |F_{LL}(u) + F_{LL}(t)|^2, \\
\frac{d\sigma}{d\Omega} (e_R^- e_R^- \rightarrow e_R^- e_R^-) &= \alpha^2 s |F_{RR}(u) + F_{RR}(t)|^2, \\
\frac{d\sigma}{d\Omega} (e_L^- e_R^- \rightarrow e_L^- e_R^-) &= \frac{\alpha^2}{s} u^2 |F_{LR}(t)|^2, \\
\frac{d\sigma}{d\Omega} (e_R^- e_L^- \rightarrow e_R^- e_L^-) &= \frac{\alpha^2}{s} u^2 |F_{RL}(t)|^2, \\
\frac{d\sigma}{d\Omega} (e_L^- e_R^- \rightarrow e_R^- e_L^-) &= \frac{\alpha^2}{s} t^2 |F_{LR}(u)|^2, \\
\frac{d\sigma}{d\Omega} (e_R^- e_L^- \rightarrow e_L^- e_R^-) &= \frac{\alpha^2}{s} t^2 |F_{RL}(u)|^2. \quad (4.20)
\end{aligned}$$

Here

$$F_{AB}(u) = \sum_{i=\gamma, Z_1, Z_2} D_i(u) g_{Ae}^i g_{Be}^i \quad (A, B = L, R).$$

If the polarizations of the final particles are not measured, the process (4.2) is characterized by the four amplitudes

$$\begin{aligned}
\frac{d\sigma}{d\Omega} (e_L^- e_L^- \rightarrow e^- e^-) &= \alpha^2 s |F_{LL}(u) + |F_{LL}(t)|^2, \\
\frac{d\sigma}{d\Omega} (e_R^- e_R^- \rightarrow e^- e^-) &= \alpha^2 s |F_{RR}(u) + |F_{RR}(t)|^2, \\
\frac{d\sigma}{d\Omega} (e_L^- e_R^- \rightarrow e^- e^-) &= \frac{\alpha^2}{2} [u^2 |F_{LR}(t)|^2 + t^2 |F_{LR}(u)|^2], \\
\frac{d\sigma}{d\Omega} (e_R^- e_L^- \rightarrow e^- e^-) &= \frac{\alpha^2}{2} [u^2 |F_{RL}(t)|^2 + t^2 |F_{RL}(u)|^2]. \quad (4.21)
\end{aligned}$$

The most general expression for the differential cross section of the reaction $e^- e^- \rightarrow e^- e^-$ with allowance for the longitudinal polarizations of all the particles can be represented in the form²³

$$\begin{aligned}
\frac{d\sigma}{d\Omega} &= \frac{\alpha^2}{16s} \{ s^2 [|F_{LL}(u) + F_{LL}(t)|^2 (1 - \lambda_1)(1 - \lambda_2) \\
&\quad \times (1 - h_1)(1 - h_2) + |F_{RR}(u) \\
&\quad + F_{RR}(t)|^2 (1 + \lambda_1)(1 + \lambda_2)(1 + h_1)(1 + h_2)] \\
&\quad + u^2 |F_{LR}(t)|^2 [(1 - \lambda_1)(1 + \lambda_2)(1 - h_1)(1 + h_2) \\
&\quad + (1 + \lambda_1)(1 - \lambda_2)(1 + h_1)(1 - h_2)] \\
&\quad + t^2 |F_{LR}(u)|^2 [(1 - \lambda_1)(1 + \lambda_2)(1 + h_1)(1 - h_2) \\
&\quad + (1 + \lambda_1)(1 - \lambda_2)(1 - h_1)(1 + h_2)] \}. \quad (4.22)
\end{aligned}$$

Here λ_1 and λ_2 (respectively, h_1 and h_2) are the helicities of the electrons before (after) the scattering.

Using the expression (4.22), we can obtain the following expressions for the polarization characteristics of the process that can be measured experimentally:

$$A_{RL} = \frac{d\sigma_R - d\sigma_L}{d\sigma_R + d\sigma_L} = \frac{C_4}{C_1 + C_2 + C_3}, \quad (4.23)$$

$$A_{\lambda_1} = \frac{1}{\lambda_1} \cdot \frac{d\sigma(\lambda_1) - d\sigma(-\lambda_1)}{d\sigma(\lambda_1) + d\sigma(-\lambda_1)} = A_{\lambda_2} = A_{RL}, \quad (4.24)$$

$$\begin{aligned}
A_{\lambda_1 \lambda_2} &= \frac{d\sigma(\lambda_1, \lambda_2) - d\sigma(-\lambda_1, -\lambda_2)}{d\sigma(\lambda_1, \lambda_2) + d\sigma(-\lambda_1, -\lambda_2)} \\
&= \frac{(\lambda_1 + \lambda_2) C_4}{(C_1 + C_3)(1 + \lambda_1 \lambda_2) + C_2(1 - \lambda_1 \lambda_2)}, \quad (4.25)
\end{aligned}$$

$$\tilde{A}_{\lambda_1 \lambda_2} = \frac{1}{\lambda_1 \lambda_2} + \frac{d\sigma(\lambda_1, \lambda_2) - d\sigma(-\lambda_1, \lambda_2) - d\sigma(\lambda_1, -\lambda_2) + d\sigma(-\lambda_1, -\lambda_2)}{d\sigma(\lambda_1, \lambda_2) + d\sigma(-\lambda_1, \lambda_2) + d\sigma(\lambda_1, -\lambda_2) + d\sigma(-\lambda_1, -\lambda_2)} = (C_1 - C_2 + C_3) / (C_1 + C_2 + C_3), \quad (4.26)$$

$$N_\lambda = \frac{d\sigma(\lambda_1) - d\sigma(\lambda_1 = 0)}{d\sigma(\lambda_1) + d\sigma(\lambda_1 = 0)} = \frac{\lambda_1 C_4}{2(C_1 + C_2 + C_3) + \lambda_1 C_4}, \quad (4.27)$$

$$P = \frac{d\sigma(h_1 = 1) - d\sigma(h_1 = -1)}{d\sigma(h_1 = 1) + d\sigma(h_1 = -1)} = A_{RL}, \quad (4.28)$$

$P(\lambda_1, \lambda_2)$

$$= \frac{d\sigma(\lambda_1, \lambda_2, h_1 = 1) - d\sigma(\lambda_1, \lambda_2, h_1 = -1)}{d\sigma(\lambda_1, \lambda_2, h_1 = 1) + d\sigma(\lambda_1, \lambda_2, h_1 = -1)}$$

$$\begin{aligned}
&= \frac{(C_1 - C_2)(\lambda_1 - \lambda_2) + C_3(\lambda_1 + \lambda_2) + C_4(1 + \lambda_1 \lambda_2)}{(C_1 + C_2)(1 - \lambda_1 \lambda_2) + C_3(1 + \lambda_1 \lambda_2) + C_4(\lambda_1 + \lambda_2)}. \quad (4.29)
\end{aligned}$$

Here we have introduced the notation

$$C_1 = 2u^2 |F_{LR}(t)|^2, \quad C_2 = 2t^2 |F_{LR}(u)|^2,$$

$$C_{3,4} = s^2 [|F_{RR}(t) + F_{RR}(u)|^2 \pm |F_{LL}(t) + F_{LL}(u)|^2].$$

It follows from (29) that in the case of scattering of electrons with the same helicities ($\lambda_1 = \lambda_2$) the degree of longitudinal polarization of the electron is

$$P(\lambda_1 = \lambda_2 = \pm 1) = \pm 1,$$

i.e., if the spins of the electrons are originally antiparallel, then the scattered electrons remain completely longitudinally polarized. The same result was obtained in Ref. 59 in the case of the electromagnetic mechanism of $e^-e^- \rightarrow e^-e^-$ scattering.

We made calculations of the polarization characteristics of the processes (4.1) and (4.2) for Z - Z' mixing angles $\Phi = -0.1, -0.05, 0, 0.05$, and 0.1 rad. For the electron scattering angle, the value $\theta = 90^\circ$ was chosen.

Figure 7 shows the energy dependence of the right-left asymmetry A_{RL} for $\theta_E = 90^\circ$, $\Phi = 0.1$ rad, and different masses M_{Z_2} . It can be seen that in the standard model the asymmetry A_{RL} in the reaction $e^-e^+ \rightarrow e^-e^+$ increases in absolute magnitude with increasing energy and reaches a maximum at the Z peak (at $\sqrt{s} = M_Z$), after which A_{RL} decreases and vanishes at the energy $\sqrt{s} = 1.15M_Z$. On going through the point $\sqrt{s} = 2M_Z$, the polarization asymmetry A_{RL} again changes sign. Observation of the predicted behavior of the asymmetry A_{RL} at high energies would be a new proof of the validity of the standard model.

In the E_6 superstring model, the zeros and the maximum of the asymmetry A_{RL} remain but are shifted to the right. The maximum of the asymmetry is observed at the Z_2 peak (at $\sqrt{s} = M_{Z_2}$). Study of the right-left asymmetry A_{RL} is of great interest for determining the mass of the additional Z' boson.

In the standard model, an increase of the energy in the case of elastic electron-electron scattering leads to a monotonic decrease of the asymmetry A_{RL} . The predictions of the E_6 model differ significantly from the results of the standard model; moreover, the deviation from the standard model increases with increasing energy of the e^-e^- (e^-e^+) beams and with decreasing mass of the additional boson.

Similar behavior is also observed for the polarization N_λ of the electron beam. The value of N_λ is very sensitive to the sign of λ_1 . For example, if $\lambda_1 = -1$, then N_λ reaches 80%, while for $\lambda_1 = 1$ we have $N_\lambda \sim 30\%$.

The transverse spin asymmetry $A_\phi^{(2)}$ is determined by the imaginary parts of the boson propagators and therefore reaches a maximum value near the resonance energy $\sqrt{s} = M_i$. At the Z pole ($\sqrt{s} \sim 90$ GeV), the asymmetry is $A_\phi^{(2)} = -0.8\%$. However, at the Z' resonance, $A_\phi^{(2)}$ reaches tens of percent and is sensitive to the mixing angles θ_E and Φ .

Note that in the standard model the right-left asymmetry A_{RL} , the transverse spin asymmetry $A_\phi^{(2)}$, and the polarization of the electron beam N_λ , which arise in the processes $e^-e^+ \rightarrow e^-e^+$ and $e^-e^- \rightarrow e^-e^-$ as a result of γ - Z interference, are proportional to the vector constant g_{ve}^Z , and for $\sin^2 \theta_w = 0.23$ they are strongly suppressed. However, in the E_6 superstring model with two bosons an additional γ - Z' interference term occurs in the asymmetries A_{RL} , $A_\phi^{(2)}$, and N_λ and plays a decisive role in the region of energies $\sqrt{s} \sim M_{Z'}$.

With regard to the asymmetries $A_\phi^{(1)}$ and $A_{\lambda_1\lambda_2}$ and the degree of longitudinal polarization $P(\lambda_1, \lambda_2)$ of the electron, they reach values of order 100% in the standard model too,

and a significant effect of the additional boson on these characteristics is observed at higher energies.

5. SUPERSTRING Z' BOSON IN $e^-e^+ \rightarrow BX$ ANNIHILATION

At the present time, the experimental and theoretical investigation of the production of hadrons in high-energy colliding e^-e^+ beams occupies a central position in elementary-particle physics. The reason for this is that it creates favorable conditions for studying the structure of the particles and testing the validity of the predictions of various composite models (quark, parton, etc.). Especially interesting are reactions of the type $e^-e^+ \rightarrow N + \text{hadrons}$, since these processes are related by crossing to the inelastic-scattering reactions $eN \rightarrow e + \text{hadrons}$ and in conjunction with them make it possible to obtain information about the structure functions of the hadrons in the complete range of variation of the square of the momentum transfer.

In this section, we study the effects of the superstring Z' boson in inclusive annihilation of a longitudinally polarized e^-e^+ pair into hadrons with one distinguished baryon B in the final state with polarization measured in the experiment (Refs. 22 and 24):

$$e^- + e^+ \rightarrow (\gamma, Z_1, Z_2, \dots) \rightarrow B + X. \quad (5.1)$$

Here X is the system of undetected hadrons.

The process of inclusive production of the baryon B with 4-momentum P and helicity h in e^-e^+ annihilation is described by the matrix element

$$M = e^2 \sum_i \bar{v} \gamma_\mu [G_L^i (1 + \gamma_5) + G_R^i (1 - \gamma_5)] u(B(p, h) X | J_\mu^i | 0), \quad (5.2)$$

where $G_{L(R)}^i = g_{L(R)e}^i D_i(s)$; the summation is over all the gauge bosons $i = \gamma, Z_1, Z_2$ (in what follows, the summation sign is omitted); J_μ^i is the hadron current that describes the transition $i \rightarrow BX$.

The differential cross section of the reaction (5.1) can be represented in the form

$$\frac{d\sigma}{d\Omega} = \frac{\alpha^2}{4} \beta x dx L_{\mu\nu}^{ik} \bar{H}_{\mu\nu}^{ik}, \quad (5.3)$$

where $x = 2E_B / \sqrt{s}$ is the energy of the baryon in units of the electron energy; β and $\Omega(\theta, \varphi)$ are the velocity and solid angle of emission of the baryon; $L_{\mu\nu}^{ik}$ and $\bar{H}_{\mu\nu}^{ik}$ are the lepton and hadron tensors. The bar over the tensor $H_{\mu\nu}^{ik}$ indicates a summation over the polarizations and an integration over the momenta of the undetected hadrons:

$$\bar{H}_{\mu\nu}^{ik} (2\pi)^3 \int \langle B(p, h) X | J_\mu^i | 0 \rangle \langle B(p, h) X | J_\nu^k | 0 \rangle^* \delta(q - p - p_x) d\Phi_x. \quad (5.4)$$

Here q is the 4-momentum transfer to the hadrons; p_x and $d\Phi_x$ are the total 4-momentum and phase space of the hadronic system X .

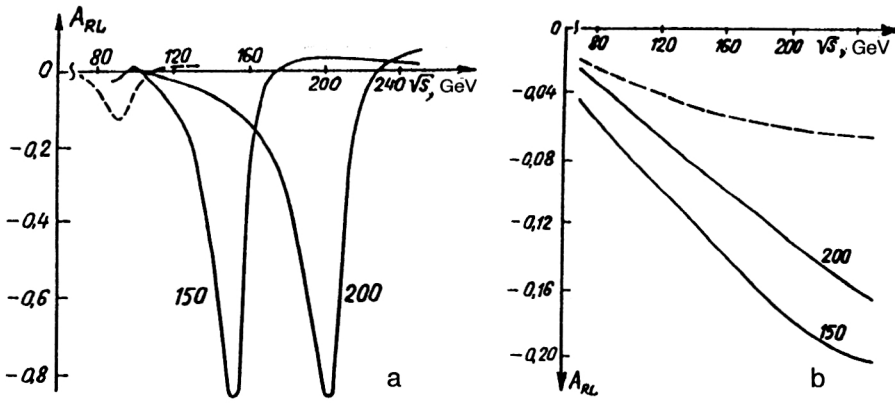


FIG. 7. Dependence of the asymmetry A_{RL} on the energy in the processes (a) $e^-e^+ \rightarrow e^-e^+$ and (b) $e^-e^- \rightarrow e^-e^-$ for $\Phi=0.1$ rad, $\theta_E=90^\circ$, and different masses of the Z_2 boson (the numbers next to the curves give the mass M_{Z_2} in giga-electron-volts). The dashed curves describe the predictions of the standard model.

It follows from (5.4) that the tensor $\bar{H}_{\mu\nu}^{ik}$ depends on the baryon helicity h and on the 4-momenta p and q , and is the sum of a tensor and a pseudotensor. In the general case, the tensor $\bar{H}_{\mu\nu}^{ik}$ is given by

$$\begin{aligned} \bar{H}_{\mu\nu}^{ik} = & (W_1^{ik} + hT_1^{ik})(\delta_{\mu\nu} - q_\mu q_\nu / q^2) \\ & - (W_2^{ik} + hT_2^{ik}) \frac{1}{q^2} \left(q_\mu - p_\mu \frac{q^2}{p \cdot q} \right) \left(q_\nu - q_\nu \frac{q^2}{p \cdot q} \right) \\ & + (W_3^{ik} + hT_3^{ik}) \varepsilon_{\mu\nu\rho\sigma} p_\rho q_\sigma / p \cdot q + (W_4^{ik} \\ & + hT_4^{ik}) q_\mu q_\nu / q^2 + (W_5^{ik} + hT_5^{ik})(p_\mu q_\nu + p_\nu q_\mu) / p \cdot q \\ & + (W_6^{ik} + hT_6^{ik})(p_\mu q_\nu - p_\nu q_\mu) / p \cdot q. \end{aligned} \quad (5.5)$$

Here W_r^{ik} and T_r^{ik} ($r=1, \dots, 6$) are the structure functions of the hadrons, which depend on the two invariants s and $\nu = -pq$ (or s and $x = -2\nu/s$). Among them, $W_{1,2,4,5,6}^{ik}$ and T_3^{ik} conserve P invariance, while W_3^{ik} and $T_{1,2,4,5,6}^{ik}$ violate it.

In the limit of vanishing electron mass, the lepton tensors are conserved, $L_{\mu\nu}^{ik} q_\mu = L_{\mu\nu}^{ik} q_\nu = 0$, and therefore the structure functions $W_{4,5,6}^{ik}$ and $T_{4,5,6}^{ik}$ do not contribute to the cross section. As a result, the cross section of the process (5.1) is determined by the structure functions $W_{1,2,3}^{ik}$ and $T_{1,2,3}^{ik}$:

$$\begin{aligned} \frac{d\sigma}{d\Omega dx} = & \frac{\alpha^2}{4} s \beta x \{ [g_1^{ik}(1 - \lambda_1 \lambda_2) + g_2^{ik}(\lambda_2 - \lambda_1)] \\ & \times [2(W_1^{ik} + hT_1^{ik}) + (W_2^{ik} + hT_2^{ik})\beta^2 \sin^2 \theta] \\ & + 2[g_2^{ik}(1 - \lambda_1 \lambda_2) + g_1^{ik}(\lambda_2 - \lambda_1)](W_3^{ik} \\ & + hT_3^{ik})\beta \cos \theta - \eta_1 \eta_2 (g_3^{ik} \cos 2\varphi \\ & + i g_4^{ik} \sin 2\varphi)(W_2^{ik} + hT_2^{ik})\beta^2 \sin^2 \theta \}, \end{aligned} \quad (5.6)$$

where

$$g_{1(2)}^{ik} = G_L^i G_L^{*k} \pm G_R^i G_R^{*k}; \quad g_{3(4)}^{ik} = G_R^i G_L^{*k} \pm G_L^i G_R^{*k}.$$

If the electron (positron) has right-handed (left-handed) helicity, then from the expression (5.6) we obtain the cross section

$$\frac{d\sigma}{d\Omega dx} (e^- e_L^+ \rightarrow BX) = \alpha^2 s \beta x G_R^i G_R^{*k} [2W_1^{ik}$$

$$\begin{aligned} & + W_2^{ik} \beta^2 \sin^2 \theta - 2W_3^{ik} \beta \cos \theta \\ & + h(2T_1^{ik} + T_2^{ik} \beta^2 \sin^2 \theta \\ & - 2T_3^{ik} \beta \cos \theta)]. \end{aligned} \quad (5.7)$$

If, however, the electron (positron) has left-handed (respectively, right-handed) polarization, then the cross section is

$$\begin{aligned} \frac{d\sigma}{d\Omega dx} (e_L^- e_R^+ \rightarrow BX) = & \alpha^2 s \beta x G_L^i G_L^{*k} [2W_1^{ik} \\ & + W_2^{ik} \beta^2 \sin^2 \theta + 2W_3^{ik} \beta \cos \theta \\ & + h(2T_1^{ik} + T_2^{ik} \beta^2 \sin^2 \theta \\ & + 2T_3^{ik} \beta \cos \theta)]. \end{aligned} \quad (5.8)$$

It follows from this that study of the reactions (5.1) with left-polarized electrons e_L^- (or right-polarized positrons e_R^+) makes it possible to obtain information about the left coupling constants with the gauge bosons, g_{Le}^i , whereas the cross section for annihilation of right-polarized electrons e_R^- (or left-polarized positrons e_L^+) contains information about the right coupling constants g_{Re}^i .

We find the structure functions in the quark-parton model, in accordance with which the process (5.1) takes place in two stages. First, a quark-antiquark pair is produced by a gauge boson i , and the pair then fragments into hadrons. We assume that in the final state a fast baryon B carrying the fraction $x = E_B/E_q = 2E_B/\sqrt{s} \sim 1$ of the quark momentum is detected. It is natural to assume that such a baryon is formed from a fast quark emitted in the same direction—the fast quark captures the missing quarks from the sea and forms the fast baryon B .

The differential cross section of the reaction (5.1) in the quark-parton model can be written in the form

$$\frac{d\sigma}{dx d\Omega} = \sum_{q, h_q} \frac{d\sigma_q(h_q)}{d\Omega_q} D_{q, h_q}^{B, h}(x) + \sum_{\bar{q}, h_{\bar{q}}} \frac{d\sigma_{\bar{q}}(h_{\bar{q}})}{d\Omega_{\bar{q}}} D_{\bar{q}, h_{\bar{q}}}^{B, h}(x). \quad (5.9)$$

Here the sum is over all quark flavors: $D_{q, h_q}^{B, h}(x)$ [$D_{\bar{q}, h_{\bar{q}}}^{B, h}(x)$] is the function of fragmentation of a quark (respectively, antiquark) with helicity h_q ($h_{\bar{q}}$) into a baryon with longitudinal

polarization h , and the differential cross section of the elementary subprocess $e^-e^+ \rightarrow (\gamma, Z_1, Z_2) \rightarrow q\bar{q}$, which determines the angular distribution of the longitudinally polarized quarks, has the form

$$\begin{aligned} \frac{d\sigma_q(h_q)}{d\Omega_q} = & \frac{\alpha^2 N_c s}{2} \{ [g_1^{ik}(1 - \lambda_1 \lambda_2) + g_2^{ik}(\lambda_2 - \lambda_1)] \\ & \times (q_1^{ik} - h_q q_2^{ik})(1 + \cos^2 \theta) \\ & + 2[g_2^{ik}(1 - \lambda_1 \lambda_2) + g_1^{ik}(\lambda_2 - \lambda_1)](q_2^{ik} \\ & - h_q q_1^{ik}) \cos \theta - \eta_1 \eta_2 [g_3^{ik} \cos 2\varphi \\ & + i g_q^{ik} \sin 2\varphi](q_1^{ik} - h_q q_2^{ik}) \sin^2 \theta \}, \end{aligned} \quad (5.10)$$

where

$$q_{1(2)}^{ik} = g_{Lq}^i q_{Lq}^k \pm g_{Rq}^i q_{Rq}^k,$$

$N_c=3$ is the color factor, and g_{Lq}^i and g_{Rq}^i are the chiral constants of the weak neutral current of the quark.

The angular distribution of the longitudinally polarized antiquarks is obtained from (5.10) by means of the substitutions $h_q \rightarrow -h_{\bar{q}}$, $\theta \rightarrow \pi - \theta$.

Conservation of P in the fragmentation process leads to the relations

$$D_{q,-h_q}^{B,-h}(x) = D_{q,h_q}^{B,h}(x).$$

For brevity, we introduce the notation

$$D_q^B(x) \equiv D_{q,+1}^{B,+1}(x) + D_{q,-1}^{B,-1}(x),$$

$$\Delta_q^B(x) \equiv D_{q,+1}^{B,+1}(x) - D_{q,-1}^{B,-1}(x).$$

From comparison of the expressions (5.6) and (5.9) with allowance for the angular distributions of the quarks (5.10) and antiquarks, we obtain for the structure functions of the hadrons the expressions (the baryon mass is ignored)

$$\begin{aligned} xW_1^{ik} &= -xW_2^{ik} = 2N_c \sum_q q_1^{ik} [D_q^B(x) + D_{\bar{q}}^B(x)], \\ xW_3^{ik} &= 2N_c \sum_q q_2^{ik} [D_q^B(x) - D_{\bar{q}}^B(x)], \\ xT_1^{ik} &= -xT_2^{ik} = 2N_c \sum_q q_2^{ik} [\Delta_q^B(x) - \Delta_{\bar{q}}^B(x)], \\ xT_3^{ik} &= 2N_c \sum_q q_1^{ik} [\Delta_q^B(x) + \Delta_{\bar{q}}^B(x)]. \end{aligned} \quad (5.11)$$

In the case of annihilation of longitudinally polarized positrons, the differential cross section of the process (5.1) has the form (here we take into account the relations $W_2^{ik} = -W_1^{ik}$ and $T_2^{ik} = -T_1^{ik}$, which are predicted by the quark-parton model)

$$\begin{aligned} \frac{d\sigma}{dx d\Omega} = & \frac{\alpha^2 s}{4} g_1^{ik} W_1^{ik} (1 + \cos^2 \theta) [1 + A_{FB}(s, x, \theta)] [1 \\ & + \lambda_2 A_{RL}(s, x, \theta) + h P_B(s, x, \theta)], \end{aligned} \quad (5.12)$$

where $A_{FB}(s, x, \theta)$, $A_{RL}(s, x, \theta)$, and $P_B(s, x, \theta)$ are the forward-backward angular asymmetry, the right-left asym-

metry, and the degree of longitudinal polarization of the baryon. Measured experimentally, these differential characteristics are determined by the expressions

$$A_{FB}(s, x, \theta) = A_{FB}(s, x) f(\theta), \quad (5.13)$$

$$A_{RL}(s, x, \theta) = \frac{A_{RL}^{(1)}(s, x) + A_{RL}^{(2)}(s, x) f(\theta)}{1 + A_{FB}(s, x) f(\theta)}, \quad (5.14)$$

$$P_B(s, x, \theta) = \frac{P_B^{(1)}(s, x) + P_B^{(2)}(s, x) f(\theta)}{1 + A_{FB}(s, x) f(\theta)}. \quad (5.15)$$

Here

$$f(\theta) = 2 \cos \theta / (1 + \cos^2 \theta),$$

$$A_{FB}(s, x) = g_2^{ik} W_3^{ik} / g_1^{ik} W_1^{ik},$$

$$A_{RL}^{(1)}(s, x) = g_2^{ik} W_1^{ik} / g_1^{ik} W_1^{ik}; \quad A_{RL}^{(2)}(s, x) = g_1^{ik} W_3^{ik} / g_1^{ik} W_1^{ik},$$

$$P_B^{(1)}(s, x) = -g_1^{ik} T_1^{ik} / g_1^{ik} W_1^{ik}, \quad P_B^{(2)}(s, x) = -g_2^{ik} T_3^{ik} / g_1^{ik} W_1^{ik}.$$

Experimental study of the angular and energy dependences of the asymmetries $A_{FB}(s, x, \theta)$ and $A_{RL}(s, x, \theta)$ and of the degree of longitudinal polarization $P_B(s, x, \theta)$ of the baryon is a source of information about the chiral coupling constants of the quark weak neutral currents and about the functions for fragmentation of quarks into baryons.

At the present time, the functions for fragmentation of polarized quarks into polarized baryons are completely unknown. Therefore, for quantitative estimates of the main characteristics of the $e^-e^+ \rightarrow \Lambda^0 X$ and $e^-e^+ \rightarrow \Sigma^+ X$ processes we shall proceed from the model used in Ref. 46. We are particularly interested in the degree of longitudinal polarization of fast Λ^0 and Σ^+ hyperons, which can be readily observed using the angular asymmetry of the decays $\Lambda, \Sigma \rightarrow N\pi$.

In accordance with Ref. 46, the polarization of the fast Λ^0 and Σ^+ hyperons is determined by the expressions

$$\begin{aligned} h_\Lambda &= h_s, \\ \frac{1 + h_{\Sigma^+}}{1 - h_{\Sigma^+}} &= \frac{5Q_u^2(1 + h_u) + Q_s^2(1 + h_s)}{5Q_u^2(1 - h_u) + Q_s^2(1 - h_s)}, \end{aligned} \quad (5.16)$$

where h_u and h_s (respectively, Q_u and Q_s) are the polarizations (charges) of the u and s quarks.

Exact $SU(6)$ symmetry leads to the following values for the baryon helicities:⁴⁶

$$\begin{aligned} \frac{1 + h_\Lambda}{1 - h_\Lambda} &= \frac{Q_u^2 + Q_d^2 + Q_s^2(1 + h_s)}{Q_u^2 + Q_d^2 + Q_s^2(1 - h_s)}, \\ \frac{1 + h_{\Sigma^+}}{1 - h_{\Sigma^+}} &= \frac{Q_u^2[5(1 + h_u) + (1 - h_u)] + Q_s^2[(1 + h_s) + 2(1 - h_s)]}{Q_u^2[5(1 - h_u) + (1 + h_u)] + Q_s^2[(1 - h_s) + 2(1 + h_s)]}. \end{aligned} \quad (5.17)$$

With regard to the polarizations of baryons containing heavy quarks, we assume, following Ref. 47, that in the case when in the reaction $e^-e^+ \rightarrow \text{hadrons}$ there is production of a fast charmed baryon B_c or a beauty baryon B_b with $x \sim 1$, the

TABLE VI. Values of the polarizations $P_B^{(1)}$ and $P_B^{(2)}$ at resonance.

Process	Model	Z resonance		Z' resonance ($\theta_E=90^\circ$)	
		$P_B^{(1)}$	$P_B^{(2)}$	$P_B^{(1)}$	$P_B^{(2)}$
$e^-e^+ \rightarrow \tau^- \tau^+$		-0.16	-0.16	-0.8	-0.8
$e^-e^+ \rightarrow \Lambda^0 X$	[46]	-0.94	-0.16	0.8	-0.8
	[47]	-0.88	-0.16	0.73	-0.8
	SU(6)	-0.16	-0.03	0.13	-0.13
$e^-e^+ \rightarrow \Sigma^+ X$	[46]	-0.68	-0.16	0.04	-0.72
	[47]	-0.78	-0.16	0.57	-0.8
	SU(6)	-0.36	-0.08	-0.03	-0.44
$e^-e^+ \rightarrow \Sigma^- X$	[47]	-0.94	-0.16	0.8	-0.8
$e^-e^+ \rightarrow B_c X$	[47]	-0.67	-0.16	0	-0.8
$e^-e^+ \rightarrow B_b X$	[47]	-0.94	-0.16	0.8	-0.8

longitudinal polarization of a heavy c or b quark is transferred to it, i.e., in the production of B_c or B_b baryons the contribution of the c or b quarks to the fragmentation function dominates over the contribution of the light quarks:

$$D_{Q,h_Q}^{B,h}(x) \gg D_{q,h_q}^{B,h}(x), \quad Q=c,b, \quad q=u,d,s.$$

In Table VI, we give the values of the polarizations $P_B^{(1)}$ and $P_B^{(2)}$ in the Z or Z' resonance region of energies ($s=M_i^2$) for the value $x_W=0.23$ of the Weinberg parameter. It can be seen that the results of the models of Ref. 46 and Ref. 47 differ by only a few percent (an exception is the value of the polarization $P_\Sigma^{(1)}$ at the Z' resonance). Exact SU(6) symmetry leads to values of the polarizations $P_B^{(1)}$ and $P_B^{(2)}$ for the Λ^0 and Σ^+ hyperons that are too low.

Figures 8 and 9 give the energy dependences of the longitudinal polarization of the Λ^0 and Σ^+ hyperons for different masses of the additional boson. The dashed curves illustrate the behavior of the polarizations in the standard model for $x_W=0.23$. It can be seen that for the fixed mass value $M_{Z'}=150$ GeV the degrees of longitudinal polarization $P_\Lambda^{(1)}$ and $P_\Sigma^{(1)}$ increase with increasing energy of the e^-e^+ beams and, having reached a maximum value near $\sqrt{s} \sim 140$ GeV, then begin to decrease. The increase in the mass of the additional boson does not change the nature of the dependence of the degree of longitudinal polarization on the energy, but its maximum is shifted to higher energies.

We now consider the integrated characteristics of the process (5.1). We define the cross sections for production of baryon B in the forward and backward hemispheres in the case of annihilation of a polarized positron and an unpolarized electron as follows:

$$\sigma_F(\lambda_2) = \int_0^1 dx \int_0^{2\pi} d\varphi \int_0^1 d \cos \theta (d\sigma/dxd\Omega),$$

$$\sigma_B(\lambda_2) = \int_0^1 dx \int_0^{2\pi} d\varphi \int_{-1}^0 d \cos \theta (d\sigma/dxd\Omega). \quad (5.18)$$

From the expression (5.6), we have

$$\sigma_{F(B)}(\lambda_2) = \frac{\pi\alpha^2 s}{3} [4(g_1^{ik} + \lambda_2 g_2^{ik})I_1^{ik} \pm 3(g_2^{ik} \pm \lambda_2 g_1^{ik})I_3^{ik}], \quad (5.19)$$

where

$$I_n^{ik} = \int_0^1 x W_n^{ik} dx, \quad n=1,3.$$

The expression (5.19) leads to the following electroweak asymmetries:

1) the forward (backward) polarization asymmetry

$$A_{F(B)}(\lambda_2) = \frac{\sigma_{F(B)}(\lambda_2) - \sigma_{F(B)}(\lambda_2)}{\sigma_{F(B)}(\lambda_2) + \sigma_{F(B)}(\lambda_2)} = \lambda_2 \times \frac{4g_2^{ik}I_1^{ik} \pm 3g_1^{ik}I_3^{ik}}{4g_1^{ik}I_1^{ik} \pm 3g_2^{ik}I_3^{ik}}; \quad (5.20)$$

2) the forward-backward asymmetry

$$A_{FB}(\lambda_2) = [\sigma_F(\lambda_2) - \sigma_B(\lambda_2)] / [\sigma_F(\lambda_2) + \sigma_B(\lambda_2)] = \frac{3}{4} \frac{(g_2^{ik} + \lambda_2 g_1^{ik})I_3^{ik}}{(g_1^{ik} + \lambda_2 g_2^{ik})I_1^{ik}}; \quad (5.21)$$

3) the forward-backward polarization asymmetry

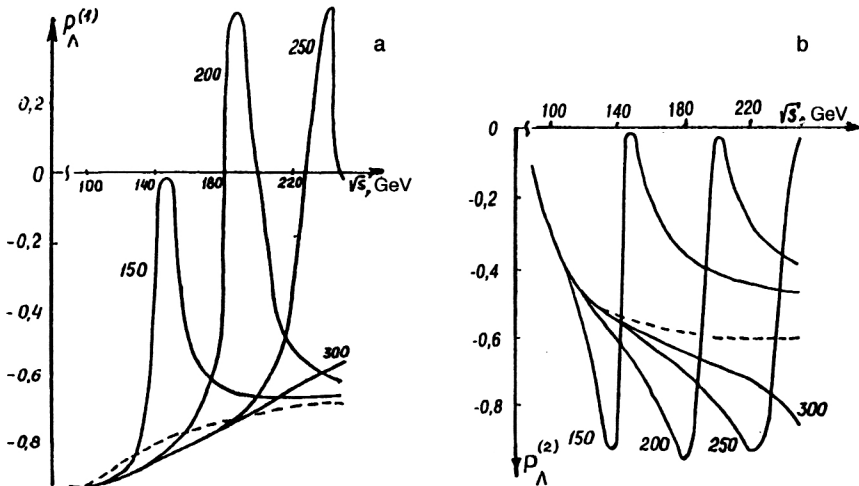


FIG. 8. Dependence of the degree of longitudinal polarization $P_\Lambda^{(1)}$ (a) and $P_\Lambda^{(2)}$ (b) on the energy in the process $e^-e^+ \rightarrow \Lambda^0 X$ for different masses of the additional boson (the numbers next to the curves give the mass $M_{Z'}$, in giga-electron-volts) and $\theta_E=0^\circ$.

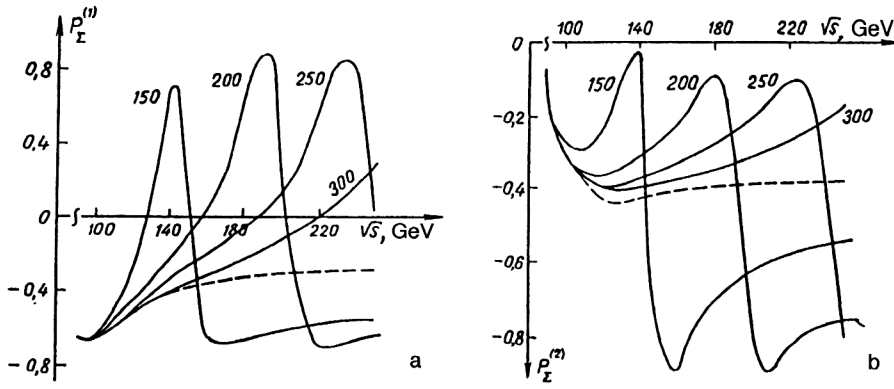


FIG. 9. Dependence of the degree of longitudinal polarization $P_z^{(1)}$ (a) and $P_z^{(2)}$ (b) on the energy in the process $e^- e^+ \rightarrow \Sigma^+ X$ for different masses M_Z and $\theta_E = 0^\circ$.

$$\begin{aligned} \tilde{A}_{FB}(\lambda_2) &= \frac{\sigma_F(\lambda_2) - \sigma_F(-\lambda_2) - \sigma_B(\lambda_2) + \sigma_B(-\lambda_2)}{\sigma_F(\lambda_2) + \sigma_F(-\lambda_2) + \sigma_B(\lambda_2) + \sigma_B(-\lambda_2)} \\ &= \frac{3}{4} \lambda_2 \cdot \frac{g_1^{ik} I_3^{ik}}{g_1^{ik} I_1^{ik}}; \end{aligned} \quad (5.22)$$

4) the right-left asymmetry

$$A_{RL} = (\sigma_R - \sigma_L) / (\sigma_R + \sigma_L) = g_2^{ik} I_1^{ik} / g_1^{ik} I_1^{ik}, \quad (5.23)$$

where $\sigma_R = \sigma_F(\lambda_2=1) + \sigma_B(\lambda_2=1)$ and $\sigma_L = \sigma_F(\lambda_2=-1) + \sigma_B(\lambda_2=-1)$ are the cross sections for annihilation of right- and left-polarized positrons.

The cross sections for annihilation of an unpolarized $e^- e^+$ pair with production of a polarized baryon in the forward and backward hemispheres are

$$\sigma_{F(B)}(h) = \frac{\pi \alpha^2 s}{6} [4g_1^{ik}(I_1^{ik} + hF_1^{ik}) \pm 3g_2^{ik}(I_3^{ik} + hF_3^{ik})]. \quad (5.24)$$

We have here introduced the notation

$$F_n^{ik} = \int_0^1 x T_n^{ik} dx, \quad n = 1, 3.$$

The expression (5.24) leads to the following polarization asymmetries:

1) forward (backward) polarization asymmetry:

$$A_{F(B)}(h) = \frac{\sigma_{F(B)}(h) - \sigma_{F(B)}(-h)}{\sigma_{F(B)}(h) + \sigma_{F(B)}(-h)} = h \frac{4g_1^{ik} F_1^{ik} \pm 3g_2^{ik} F_3^{ik}}{4g_1^{ik} I_1^{ik} \pm 3g_2^{ik} I_3^{ik}}; \quad (5.25)$$

2) forward-backward asymmetry in the production of a polarized baryon:

$$A_{FB}(h) = \frac{\sigma_F(h) - \sigma_B(h)}{\sigma_F(h) + \sigma_B(h)} = \frac{3g_2^{ik}(I_3^{ik} + hF_3^{ik})}{4g_1^{ik}(I_1^{ik} + hF_1^{ik})}; \quad (5.26)$$

3) forward-backward polarization asymmetry:

$$\begin{aligned} \tilde{A}_{FB}(h) &= \frac{\sigma_F(h) - \sigma_F(-h) - \sigma_B(h) + \sigma_B(-h)}{\sigma_F(h) + \sigma_F(-h) + \sigma_B(h) + \sigma_B(-h)} \\ &= \frac{3}{4} h \cdot \frac{g_2^{ik} F_3^{ik}}{g_1^{ik} I_1^{ik}}; \end{aligned} \quad (5.27)$$

4) degree of longitudinal polarization of the baryon:

$$\begin{aligned} P_B &= \frac{\sigma_F(h=1) + \sigma_B(h=1) - \sigma_F(h=-1) - \sigma_B(h=-1)}{\sigma_F(h=1) + \sigma_B(h=1) + \sigma_F(h=-1) + \sigma_B(h=-1)} \\ &= \frac{g_1^{ik} F_1^{ik}}{g_1^{ik} I_1^{ik}}. \end{aligned} \quad (5.28)$$

In the case of annihilation of a transversely polarized $e^- e^+$ pair, the cross section (5.6) leads to the spin asymmetries

$$\begin{aligned} A_\varphi^{(1)} &= \frac{2}{\eta_1 \eta_2} \int_0^1 dx \int_0^{2\pi} \cos 2\varphi d\varphi \int_{-1}^1 d \cos \theta \left(\frac{d\sigma}{dx d\Omega} \right) / \\ &\quad \int_0^1 dx \int_0^{2\pi} d\varphi \int_{-1}^1 d \cos \theta \left(\frac{d\sigma}{dx d\Omega} \right) = -g_3^{ik} I_1^{ik} / \\ &\quad (2g_1^{ik} I_1^{ik}); \end{aligned} \quad (5.29)$$

$$\begin{aligned} A_\varphi^{(2)} &= \frac{2}{\eta_1 \eta_2} \int_0^1 dx \int_0^{2\pi} \sin 2\varphi d\varphi \int_{-1}^1 d \cos \theta \left(\frac{d\sigma}{dx d\Omega} \right) / \\ &\quad \int_0^1 dx \int_0^{2\pi} d\varphi \int_{-1}^1 d \cos \theta \left(\frac{d\sigma}{dx d\Omega} \right) = -ig_4^{ik} I_1^{ik} / \\ &\quad (2g_1^{ik} I_1^{ik}). \end{aligned} \quad (5.30)$$

The results of numerical estimates of the integrated characteristics of the processes $e^- e^+ \rightarrow B_c X$ and $e^- e^+ \rightarrow B_b X$ are given in Refs. 22 and 24. Here we merely list some of the specific properties of the integrated polarization characteristics:

- 1) if the energies of the colliding $e^- e^+$ beams are $\sqrt{s} \geq 140$ GeV, the behavior of the polarization characteristics depend strongly on the mixing angle θ_E ;
- 2) the asymmetries reach maximum or minimum values near the threshold for production of the gauge Z' boson;
- 3) with increasing mass of the additional boson, the maxima and minima of the asymmetries are shifted to higher energies;
- 4) the predictions of the E_6 superstring model differ strongly from the results of the standard model at $\sqrt{s} > 100$ GeV.

CONCLUSIONS

The electroweak asymmetries A_{FB} , $A_F(\lambda_2)$, $A_B(\lambda_2)$, $A_{FB}(\lambda_2)$, $\tilde{A}_{FB}(\lambda_2)$, A_{RL} , $A_F(h)$, $A_B(h)$, $A_\phi^{(1)}$, etc., in the processes $e^-e^+ \rightarrow f\bar{f}$, $e^-e^+ \rightarrow f\bar{f}$, $e^-e^+ \rightarrow q\bar{q}g$, $e^-e^+ \rightarrow \tilde{q}\bar{\tilde{q}}g$, $e^-e^+ \rightarrow e^-e^+$, $e^-e^- \rightarrow e^-e^-$, $e^-e^+ \rightarrow BX$ are experimentally observable quantities. These effects are certainly accessible to study in the e^-e^+ colliders SLC and LEP, and in the near future the large amount of information will make it possible to test several relationships between observable quantities in the above processes.

Our analysis shows that in the standard model the helicity amplitudes and the electroweak asymmetries of the processes $e^-e^+ \rightarrow f\bar{f}$, $e^-e^+ \rightarrow f\bar{f}$, $e^-e^+ \rightarrow q\bar{q}g$, $e^-e^+ \rightarrow \tilde{q}\bar{\tilde{q}}g$ vanish at certain energies of the colliding e^-e^+ beams. The vanishing of the helicity amplitudes and of the electroweak asymmetries of the processes listed above is an as yet unverified prediction of the standard model. Observation of the predicted behavior of the asymmetries would be a new proof of the validity of the model. Violation of the corresponding predictions of the standard model would make it necessary to go beyond this model; for example, it could be explained by an additional Z' boson. The presence of such a boson must lead to displacement of the already existing zeros and to the appearance of additional zeros in the characteristics of the processes $e^-e^+ \rightarrow f\bar{f}$, $e^-e^+ \rightarrow f\bar{f}$, etc., the positions of which are determined both by the mass of the Z' boson and by the constants of its coupling to other particles. However, it should be noted that in an accurate analysis of the data of a specific experiment it is necessary to correct the results given above with allowance for all radiative corrections. For example, allowance for the width of the Z boson leads to elimination of the zeros of the helicity amplitudes, although the zeros in the asymmetries remain, of course.

As follows from our analysis, the considered polarization characteristics of the processes $e^-e^+ \rightarrow f\bar{f}$, $e^-e^+ \rightarrow f\bar{f}$, $e^-e^+ \rightarrow e^-e^+$, $e^-e^- \rightarrow e^-e^-$, $e^-e^+ \rightarrow BX$ are sensitive to the parameters of the additional Z' boson (the mass $M_{Z'}$, the width $\Gamma_{Z'}$, the chiral coupling constants $g_{L_f}^{Z'}$ and $g_{R_f}^{Z'}$, and the mixing angles θ_E and Φ), and therefore study of these characteristics will make it possible to test thoroughly the standard model at high energies, to indicate ways in which it could be extended, and to assist in establishing whether an additional neutral Z' boson exists in nature.

APPENDIX 1

The expressions for the correlation cross sections σ_a ($a=1, \dots, 9$) for the process $e^-e^+ \rightarrow q\bar{q}g$ are

$$\sigma_1 \equiv \sigma_U = \frac{1}{2(1-x_1)(1-x_2)} [x_1^2(1+n_{1z}^2) + x_2^2(1+n_{2z}^2)],$$

$$\sigma_2 \equiv \sigma_L = \frac{1}{2(1-x_1)(1-x_2)} [x_1^2(1-n_{1z}^2) + x_2^2(1-n_{2z}^2)],$$

$$\sigma_3 \equiv \sigma_T = \frac{1}{2} \sigma_L,$$

$$\sigma_4 = \sigma_5 = \sigma_9 = 0,$$

$$\sigma_6 = \frac{1}{2\sqrt{2}(1-x_1)(1-x_2)} (x_1^2 n_{1x} n_{1z} + x_2^2 n_{2x} n_{2z}),$$

$$\sigma_7 = \frac{1}{(1-x_1)(1-x_2)} (x_1^2 n_{1z} - x_2^2 n_{2z}),$$

$$\sigma_8 = \frac{1}{2\sqrt{2}(1-x_1)(1-x_2)} (x_1^2 n_{1x} - x_2^2 n_{2x}).$$

Here \mathbf{n}_1 and \mathbf{n}_2 are the unit vectors along the momenta of the quark and the antiquark, and x_1 and x_2 are their scaled energies.

APPENDIX 2

The expressions for the correlation cross sections for the process $e^-e^+ \rightarrow \tilde{q}\bar{\tilde{q}}g$ are

$$\sigma_U = \frac{1}{2} \left[1 - \frac{x_1 x_2 n_{1x} n_{2x}}{(1-x_1)(1-x_2)} \right],$$

$$\sigma_L = \frac{1}{2} \left[1 - \frac{x_1 x_2 n_{1z} n_{2z}}{(1-x_1)(1-x_2)} \right],$$

$$\sigma_T = \frac{1}{4} \cdot \frac{x_1 x_2}{(1-x_1)(1-x_2)} n_{1x} n_{2x},$$

$$\sigma_I = \frac{1}{4\sqrt{2}} \frac{x_1 x_2}{(1-x_1)(1-x_2)} (n_{1x} n_{2z} + n_{1z} n_{2x}).$$

APPENDIX 3

The expressions for the correlation cross sections $\sigma_a(T)$ for the process $e^-e^+ \rightarrow \tilde{q}\bar{\tilde{q}}g$ are as follows:

1) for a scalar quark or a scalar antiquark jet

$$x_1 = T \quad (x_2 = T),$$

$$\frac{d\sigma_U}{dT} = 3T - 2,$$

$$\frac{d\sigma_L}{dT} = \frac{T}{2(1-T)} \ln \frac{2T-1}{1-T} - \frac{3T-2}{2(1-T)},$$

$$\frac{d\sigma_T}{dT} = 0,$$

$$\frac{d\sigma_I}{dT} = \frac{1}{2\sqrt{2}} \left(\frac{T}{\sqrt{1-T}} - 2\sqrt{2T-1} \right);$$

2) for a gluon jet $x_3 = T$:

$$\frac{d\sigma_U}{dT} = \frac{3T-2}{T^2} (T^2 - 2T + 2),$$

$$\frac{d\sigma_L}{dT} = \frac{1-T}{T} \ln \frac{2T-1}{1-T} - \frac{2(1-T)(3T-2)}{T^2},$$

$$\frac{d\sigma_T}{dT} = - \frac{(1-T)(3T-2)}{T^2},$$

$$\frac{d\sigma_I}{dT} = \frac{(1-T)(2-T)}{\sqrt{2}T^2} \left(\frac{T}{\sqrt{1-T}} - 2\sqrt{2T-1} \right).$$

- ¹S. L. Glashow, Nucl. Phys. **22**, 579 (1961); S. Weinberg, Phys. Rev. Lett. **19**, 1264 (1967); A. Salam, *Elementary Particle Theory* (Almqvist and Wiksell, Stockholm, 1968), p. 367.
- ²S. M. Bilenky and J. Hosek, Phys. Rep. **90**, 73 (1982).
- ³P. F. Ermolov and A. I. Mukhin, Usp. Fiz. Nauk **124**, 385 (1978) [Sov. Phys. Usp. **21**, 185 (1978)]; I. S. Tsukerman, *Elementary Particles*, No. 1 [in Russian] (Moscow, 1981).
- ⁴M. P. Rekalov, *Neutral Weak Currents* [in Russian] (Kiev, 1988).
- ⁵L. B. Okun, *Leptons and Quarks* (North-Holland, Amsterdam, 1982) [Russ. original, Nauka, Moscow, 1981].
- ⁶B. L. Ioffe and V. A. Khoze, Fiz. Elem. Chastits At. Yadra **9**, 118 (1978) [Sov. J. Part. Nucl. **9**, 50 (1978)].
- ⁷P. S. Isaev and V. A. Tsarev, Fiz. Elem. Chastits At. Yadra **20**, 997 (1989) [Sov. J. Part. Nucl. **20**, 419 (1989)].
- ⁸D. Yu. Bardin, *High-Precision Tests of the Standard Model* [in Russian] (Dubna, 1988).
- ⁹M. B. Green and J. H. Schwarz, Phys. Lett. **149B**, 17 (1984).
- ¹⁰D. Gross *et al.*, Phys. Rev. Lett. **54**, 502 (1985); P. Candelas *et al.*, Nucl. Phys. B **258**, 46 (1985).
- ¹¹R. W. Robinett, Phys. Rev. D **33**, 1908 (1986); M. Dine *et al.*, Nucl. Phys. B **259**, 549 (1985); T. G. Rizzo, Phys. Rev. D **34**, 1438 (1986).
- ¹²V. D. Angelopoulos *et al.*, Phys. Lett. **176B**, 203 (1986); D. London and J. Rosner, Phys. Rev. D **34**, 1530 (1986); J. Ellis *et al.*, Nucl. Phys. B **276**, 436 (1986).
- ¹³G. Belanger and S. Godfrey, Phys. Rev. D **34**, 1309 (1986); M. J. Duncan and P. Langacker, Nucl. Phys. B **277**, 285 (1986); J. L. Rosner, Phys. Rev. D **35**, 2244 (1987).
- ¹⁴I. V. Polyubin, Pis'ma Zh. Éksp. Teor. Fiz. **45**, 553 (1987) [JETP Lett. **45**, 705 (1987)]; T. M. Aliev, N. A. Guliev, and Kh. A. Mustafayev, Yad. Fiz. **50**, 1078 (1989) [Sov. J. Nucl. Phys. **50**, 672 (1989)]; T. M. Aliev and M. I. Dobrolyubov, Yad. Fiz. **50**, 1392 (1989) [Sov. J. Nucl. Phys. **50**, 864 (1989)].
- ¹⁵M. V. Altaïskii and V. A. Bednyakov, Yad. Fiz. **50**, 1398 (1989) [Sov. J. Nucl. Phys. **50**, 868 (1989)].
- ¹⁶A. A. Pankov, Yad. Fiz. **57**, 472 (1994) [Phys. At. Nucl. **57**, 444 (1994)].
- ¹⁷V. A. Bednyakov and S. G. Kovalenko, Yad. Fiz. **49**, 866 (1989) [Sov. J. Nucl. Phys. **49**, 538 (1989)]; Preprint R2-89-56 [in Russian], JINR, Dubna (1989).
- ¹⁸V. A. Bednyakov, Preprint R2-90-104 [in Russian], JINR, Dubna (1990).
- ¹⁹V. A. Bednyakov and S. G. Kovalenko, Phys. Lett. **214B**, 640 (1988); **219B**, 96 (1988); Preprint E2-88-157 [in English], JINR, Dubna (1988).
- ²⁰S. K. Abdullaev and A. I. Mukhtarov, Preprint R2-89-217 [in Russian], JINR, Dubna (1989).
- ²¹S. K. Abdullaev and A. I. Mukhtarov, Yad. Fiz. **50**, 1084 (1989) [Sov. J. Nucl. Phys. **50**, 676 (1989)].
- ²²S. K. Abdullaev and A. I. Mukhtarov, Yad. Fiz. **52**, 1455 (1990) [Sov. J. Nucl. Phys. **52**, 920 (1990)].
- ²³S. K. Abdullaev, A. I. Mukhtarov, and L. P. Aliev, Yad. Fiz. **53**, 516 (1991) [Sov. J. Nucl. Phys. **53**, 323 (1991)].
- ²⁴S. K. Abdullaev, A. I. Mukhtarov, and L. P. Aliev, Izv. Akad. Nauk SSSR, Ser. Fiz. **53**, 936 (1989).
- ²⁵S. K. Abdullaev and L. P. Aliev, Izv. Vyssh. Uchebn. Zaved. Fiz. No. 5, 78 (1989).
- ²⁶S. K. Abdullaev and L. P. Aliev, Izv. Vyssh. Uchebn. Zaved. Fiz. No. 4, 117 (1987); No. 5, 111 (1987).
- ²⁷S. K. Abdullaev, Yad. Fiz., in press [Phys. At. Nucl., in press].
- ²⁸S. K. Abdullaev, Yad. Fiz., in press [Phys. At. Nucl., in press].
- ²⁹S. K. Abdullaev and A. I. Mukhtarov, Yad. Fiz., in press [Phys. At. Nucl., in press].
- ³⁰M. Cvetič and B. W. Lynn, Phys. Rev. D **35**, 51 (1987).
- ³¹E. Fernandez *et al.*, Phys. Rev. Lett. **54**, 1620 (1985).
- ³²Collaboration AMY, KEK Preprint No. 88 (1988).
- ³³Collaboration TASSO, Z. Phys. C **40**, 163 (1988).
- ³⁴Collaboration TORAZ, Phys. Lett. **208B**, 319 (1988).
- ³⁵W. T. Ford *et al.*, Phys. Rev. D **36**, 1971 (1987).
- ³⁶D. Decamp *et al.*, Phys. Lett. **241B**, 435 (1990).
- ³⁷B. Adeva *et al.*, Phys. Lett. **237B**, 136 (1990).
- ³⁸M. Z. Akrawy *et al.*, Phys. Lett. **240B**, 497 (1990).
- ³⁹Collaboration LEP, Phys. Lett. **276B**, 247 (1992).
- ⁴⁰Collaboration L3, Preprint CERN-PPE/93-31 (1993).
- ⁴¹Collaboration ALEPH, Preprint CERN-PPE/93-40 (1993); CERN-PPE/93-39 (1993).
- ⁴²S. C. C. Ting, Preprint CERN-PPE/93-34 (1993).
- ⁴³The Working Group on LEP Energy and the LEP Collaborations ALEPH, DELPHI, L3, and OPAL, Preprint CERN-PPE/93-53 (1993).
- ⁴⁴G. S. Abrams *et al.*, Preprint SLAC-PUB-5113 (1989).
- ⁴⁵M. S. Chanowitz, Science **249**, 36 (1990).
- ⁴⁶A. V. Smilga, Yad. Fiz. **25**, 461 (1977) [Sov. J. Nucl. Phys. **25**, 249 (1977)].
- ⁴⁷J. F. Nieves, Phys. Rev. D **20**, 2775 (1979).
- ⁴⁸G. Kramer, Preprint DESY 83-086 (1983).
- ⁴⁹H. A. Olsen, P. Oslando, and I. Overbo, Nucl. Phys. B **171**, 209 (1981); **192**, 33 (1981).
- ⁵⁰G. Schierholz and D. H. Schiller, Preprint DESY 80/88 (1980).
- ⁵¹T. G. Rizzo, Phys. Rev. D **20**, 2207 (1979).
- ⁵²S. K. Abdullaev and A. I. Mukhtarov, *Collision of Particles with Nuclei, Atoms, and Molecules* (Collection of Scientific Studies) [in Russian] (Baku, 1982), p. 3.
- ⁵³H. D. Dahmen, D. H. Schiller, and D. Wahner, Nucl. Phys. B **227**, 291 (1983).
- ⁵⁴P. Chiappetta *et al.*, Nucl. Phys. B **259**, 365 (1985).
- ⁵⁵D. H. Schiller and D. Wöhner, Nucl. Phys. B **255**, 505 (1985).
- ⁵⁶S. M. Bilenky and N. P. Nedelcheva, Nucl. Phys. B **283**, 295 (1987).
- ⁵⁷M. I. Vysotskii, Usp. Fiz. Nauk **146**, 591 (1985) [Sov. Phys. Usp. **28**, 667 (1985)].
- ⁵⁸D. H. Schiller and D. Wöhner, Nucl. Phys. B **259**, 597 (1985).
- ⁵⁹A. I. Mukhtarov and Yu. S. Perov, Izv. Akad. Nauk SSSR, Ser. Fiz. **22**, 883 (1958).

Translated by Julian B. Barbour